

Multi-approach gravity field models from Swarm GPS data TN-02: Swarm Data Pre-Processing, Kinematic Baselines And Accelerometer Data

**Delft University of Technology (TU Delft)
Astronomical Institute of the University of Bern (AIUB)
Astronomical Institute Ondřejov (ASU)
Institute of Geodesy Graz (IfG)
Ohio State University (OSU)**

**Version 1
2018-04-11**

Prepared and checked:

Checked:

Aleš Bezděk 2018-04-11

João Encarnação 2018-04-11
Team Member

Approved:

Pieter Visser 2018-04-11
Project Manager

© Delft University of Technology, The Netherlands, 2017. Proprietary and intellectual rights of Delft University of Technology, The Netherlands are involved in the subject-matter of this material and all manufacturing, reproduction, use, disclosure, and sales rights pertaining to such subject-matter are expressly reserved. This material is submitted for a specific purpose as agreed in writing, and the recipient by accepting this material agrees that this material will not be used, copied, or reproduced in whole or in part nor its contents (or any part thereof) revealed in any manner or to any third party, except own staff, to meet the purpose for which it was submitted and subject to the terms of the written agreement.

Table of Contents

1 WP200: Swarm data pre-processing, KBs and accelerometer data4

1.1 Introduction..... 4

1.2 Summary of the results..... 4

 1.2.1 WP210: GPS data pre-processing algorithms.....4

 1.2.2 WP220: Trade-off between Swarm accelerometer data and non-gravitational models.....4

 1.2.3 WP230: Kinematic baselines for gravity field estimation5

1.3 Acronyms..... 6

1.4 Bibliography 6

2 WP210: GPS data pre-processing algorithms.....7

2.1 Introduction..... 7

2.2 General pre-processing procedures..... 7

 2.2.1 Astronomical Institute of the University of Bern7

 2.2.2 Institute of Geodesy Graz7

 2.2.3 Delft University of Technology.....8

2.3 Mitigating ionosphere-induced artifacts in GPS-derived Swarm gravity fields..... 8

 2.3.1 Scenarios9

 2.3.2 Analysis of November 2014 data.....9

 2.3.3 Analysis of June 2015 Swarm-A data.....13

 2.3.4 Summary.....16

2.4 Recommendations16

2.5 Acronyms.....16

2.6 Bibliography17

3 WP221: Modeled non-gravitational accelerations (ASU)19

3.1 Introduction.....19

3.2 Method19

3.3 Data – selected test months19

3.4 Conclusions20

3.5 Bibliography20

4 WP222: Modeled non-gravitational accelerations (TU Delft).....22

4.1 Objective22

4.2 Method22

4.3 Conclusions23

4.4 Bibliography23

5 WP223: Measured non-gravitational accelerations24

5.1 Introduction.....24

5.2 Methodology.....24

 5.2.1 Input accelerometer data24

 5.2.2 Calibration method.....24

5.3 Measured non-gravitational accelerations of Swarm-C25

 5.3.1 Along-track accelerometer component of Swarm-C.....25

 5.3.2 Cross-track and radial accelerometer components of Swarm-C.....28

5.4 Conclusions29

5.5 Bibliography29

6 WP220: Trade-off between Swarm accelerometer data and non-gravitational models31

6.1 Introduction.....31

Multi-approach gravity field models from Swarm GPS data

SW_TN-02_ASU_GS_0001 version 1

2019-04-09

Page 3 of 44

6.2	The Decorrelated Acceleration Approach	31
6.3	Results.....	32
6.3.1	<i>Preliminary validation of the three types of non-gravitational accelerations.....</i>	<i>32</i>
6.3.2	<i>Comparison of gravity fields using accelerometer data vs. non-gravitational models</i>	<i>32</i>
6.4	Conclusions	35
6.4.1	<i>Suggested approach.....</i>	<i>36</i>
6.5	Bibliography	37
7	WP230: Kinematic baselines for gravity field estimation	38
7.1	Introduction.....	38
7.1.1	<i>WP230: KBs for gravity field estimation.....</i>	<i>38</i>
7.2	Methodology.....	38
7.2.1	<i>WP232: Kinematic baselines produced at TU Delft.....</i>	<i>38</i>
7.2.2	<i>WP231: Kinematic baselines produced at AIUB.....</i>	<i>39</i>
7.2.3	<i>Gravity field inversion from kinematic baselines and orbits.....</i>	<i>40</i>
7.3	Results.....	41
7.4	Conclusions	43
7.5	Bibliography	43

Version history

Version 1, 2018-04-11

- Initial release

1 WP200: Swarm data pre-processing, KBs and accelerometer data

1.1 Introduction

The objective of Work Package (WP) 200 is to address Task 2 of the Statement of Work (SoW). This WP was divided into sub-WPs representing individual tasks needed in order to produce this report (TN-02). The work carried out specifically in WP200 was to:

1. Ingest the deliverables from the sub-WPs, specifically from WP210, WP220 and WP230;
2. Compile TN-02, specifically:
 - a) recommending the inclusion of measured or modelled non-gravitational accelerations in the production of the gravity field models (WP421 to WP424);
 - b) concluding on the added value of scalar KBs to the quality of the gravity field solutions, as a general guideline for future studies.

Both points 1 and 2 are addressed by this report. The summary of the obtained results is in the following subsection. The remaining Sections 2–7 provide reports on the fulfilment of the individual sub-WPs. Figures and tables are numbered consecutively, the references are separately at the end of each section.

1.2 Summary of the results

1.2.1 WP210: GPS data pre-processing algorithms

The main objective of this WP was to provide guidelines for GPS data screening or weighting strategies to efficiently mitigate ionosphere-induced artifacts in the gravity field.

Based on the work carried out to address this WP (Section 2), it can be recommended to apply a GPS data down-weighting strategy which is based on the second time derivative of the free linear combination L_{gf} of the GPS carrier phase observations on the two frequencies. Both for November 2014 and June 2015 this strategy proved efficient in removing the artifacts and in keeping a good orbit quality. For months with lower ionospheric activity, the ROTI-based approach is promising as well and, in the case of June 2015 leads to a slightly less noisy gravity field solution. For this reason, the ROTI approach is a viable alternative, particularly if it is already implemented, as is the case of the KO processing done at TU Graz. Further tests over longer time spans might be needed to further determine the overall impact of the two weighting strategies and to investigate the benefits of combining both.

1.2.2 WP220: Trade-off between Swarm accelerometer data and non-gravitational models

The main output of this WP is a recommendation on the inclusion of measured or modeled non-gravitational accelerations in the production of the Swarm monthly gravity fields by all gravity field processors (point 2a in Section 1.1).

To perform the analysis (Section 6), six test months have been selected. The Swarm monthly gravity fields computed using the accelerometer (ACC) data performed better in January–March 2015, as is indicated by lower differences relative to the corresponding GRACE monthly solutions. On the other hand, over January–March 2016, the ACC-based Swarm gravity fields

showed no obvious improvement compared to the gravity fields computed using the non-gravitational models.

Following the results described in Section 6, we suggest an analysis to be performed for every available current and future monthly Swarm GPS data set, on the basis of which an optimum non-gravitational data set is compiled and provided to all gravity field processors. Namely to compute the three types of the Swarm gravity fields, produced on the basis of the data in the along-track non-gravitational component of Swarm-C defined as (i) accelerometer measurements, (ii) non-gravitational model of ASU, and (iii) non-gravitational model of TUD respectively; to compare these three solutions to the GRACE KBR reference field. In case that no ACC data set is available, the use can be made only of the two non-gravitational models. Based on the assessment, the optimum non-gravitational data set will be compiled which will use either the accelerometer data or the data coming from one of the modeled data sets, whichever produces the best results. This whole procedure – gravity field recovery, computing the test statistic and the final compilation of the recommended non-gravitational data set – can be automated. The automated procedure will produce control figures that serve as a possible quality check.

Over the six-month test period (2015–2016), as the reference we used the standard monthly GRACE gravity fields. In spite of this, we showed that the time-variable model GOCO05s can be used as a reference to distinguish the months of better accelerometer performance in the periods, when no GRACE monthly fields are available (after June 2017 and other occasional gaps).

In order to use ACC data, this suggested approach relies on the availability of the step-corrected accelerometer data, which has been produced by ESA for selected time periods using a dedicated software tool (Siemes et al., 2016). This tool performs a semi-automatic step correction and needs a manual intervention of an operator. Due to the fact that the currently available along-track accelerometer component of Swarm-C is of better quality compared to other Swarm accelerometer data, we believe that it is sufficient to provide only this component. The step-correction procedure applied to the accelerometer data is a necessary prerequisite, otherwise the numerous hardware-related signal anomalies spoil the gravity field recovery. We note that the production of this step-corrected accelerometer has been done by ESA and as such it is external with respect to this DISC project consortium.

1.2.3 WP230: Kinematic baselines for gravity field estimation

This WP analyses the added value of kinematic baselines (KBs) to the quality of the gravity field solutions and produce a general guideline for future studies (point 2b in Sect. 1.1).

In Section 7, we present an analysis of the potential added value for gravity field inversion from GNSS data by including GNSS derived inter-satellite baselines. Two different KB solutions were computed independently by two institutes over 7 test months. The KBs have been used to generate range observations between Swarm A and C, which were then introduced into the gravity field inversion process. For comparison, also solutions solely based on kinematic orbits have been produced. Comparison to the high-low (hl)-only solutions and more accurate results

from the ITSG-Grace2016 time series revealed that the inclusion of kinematic baselines has no impact on the final results.

1.3 Acronyms

AIUB	Astronomical Institute of the University of Bern, Switzerland, www.aiub.unibe.ch
ASU	Astronomical Institute (Astronomický ústav), AVCR, www.asu.cas.cz/en
AVCR	Czech Academy of Sciences (Akademie věd České Republiky), Czech Republic, www.avcr.cz/en/
IfG	Institute of Geodesy Graz, TUG, www.itsg.tugraz.at
KO	Kinematic Orbit
OSU	Ohio State University, www.osu.edu
SoW	Statement of Work, Doc. Ref. SW-SW-DTU-GS-111_ITT1-1
TU Delft	Delft University of Technology, www.tudelft.nl
WP	Work Package

1.4 Bibliography

Siemes, C., de Teixeira da Encarnação, J., Doornbos, E., van den IJssel, J., Kraus, J., Peřestý, R., et al. (2016). Swarm accelerometer data processing from raw accelerations to thermospheric neutral densities. *Earth, Planets and Space*, 68(1), 297. doi:10.1186/s40623-016-0474-5

2 WP210: GPS data pre-processing algorithms

Author(s): Daniel Arnold (WP210)

2.1 Introduction

The purpose of this section is to address Work Package (WP) 210 of Task 2. According to the Statement of Work (SoW), this WP includes the following activities (cf. Section 4.2.2.2 in that document):

- Document the currently implemented data screening procedures of all Kinematic Orbit (KO)-producing partners
- Provide guidelines for GPS data screening or weighting strategies to efficiently mitigate ionosphere-induced artifacts in the gravity field (especially for the period prior to the Swarm GPS receiver tracking loop updates).

Section 2.2 addresses the first item, i.e., the description of the general pre-processing procedures as employed by the different partners deriving KOs for Swarm from GPS data.

Section 2.3 summarizes results of tests that have been conducted to investigate the impact of different GPS data screening and weighting strategies on the quality of GPS-only Swarm gravity field solutions. The section closes with the optimal strategy that is recommended to be tested and followed by the KO-producing partners.

2.2 General pre-processing procedures

This section gives an overview on the currently implemented and employed general KO pre-processing procedures of the different partners. These are AIUB, IfG, and TU Delft.

2.2.1 Astronomical Institute of the University of Bern

For the pre-processing of GPS carrier phase data, unpaired (i.e., single-frequency) observations are first removed, as well as short continuous observation intervals. Then, a non-parametric screening is conducted to identify large carrier phase outliers. Subsequently, an epoch-difference solution based on the ionosphere-free linear combination is performed to identify and correct cycle slips. If the cycle slip correction is not possible, or in case of clock events, new carrier phase ambiguities are set up. The phase data screening relies on good a priori LEO orbit information. It is, therefore, conducted in several iterations, where in each iteration the screened phase observations are used to improve the orbit.

2.2.2 Institute of Geodesy Graz

In a first step, cycle slips are detected in the carrier phase data. The cycle slip detection algorithm is based on the analysis of the Melbourne-Wübbena (MW) linear combination and is carried out for each continuous track of a satellite independently. Initially the total variation denoising algorithm (Condat, 2013) is used to reduce the noise in the MW linear combination. After this smoothing process, epoch differences are checked against a predefined threshold. If the difference exceeds the threshold, a cycle slip is found and new ambiguities are set up for all consecutive epochs of the track. Finally, all tracks are removed if shorter than a predefined minimum length.

Based on phase observations, the rate of Total Electron Content (TEC) index (ROTI) is computed according to (Pi et al., 1997). The Rate of TEC Index (ROTI) is computed in a moving window manner using a predefined window size for each tracked satellite individually. Within the orbit estimation process, the ROTI is then used to calculate a scale factor for the a priori weights of each observation. The function to calculate the scale factor is arbitrary, but will be only applied if the factor is greater than 1. For Swarm, the factor

$$\exp(20 \cdot \text{ROTI})$$

has been found to produce the best results in combination with a 31 second window size to compute the ROTI.

2.2.3 Delft University of Technology

For the computation of KOs, only those GPS satellites with a Signal-to-Noise Ratio (SNR) of larger than 10 are considered. The elevation cutoff angle is set to 0 degrees and a minimum of 6 GPS satellites is required for a solution. The outlier editing threshold for code and carrier phase residuals is 2 m and 3.5 cm, respectively.

Currently, no screening dedicated to ionosphere-induced artifacts is applied to the kinematic Precise Orbit Determination (POD). However, to remove the largest errors due to the ionospheric disturbances, a relative screening of the KO to the reduced-dynamic orbit (which is less affected) is used.

2.3 Mitigating ionosphere-induced artifacts in GPS-derived Swarm gravity fields

GPS signals propagating from the GPS satellite to the Swarm LEOs are dispersively affected by the free electrons in Earth's ionosphere. Swarm GPS observations are affected by ionospheric scintillation, resulting in significantly larger carrier phase residuals over the geomagnetic poles and around the geomagnetic equator (IJssel et al., 2015). Jäggi et al. (2016) have confirmed this clear geographical dependency for the kinematic orbit solutions processed at AIUB and showed that in particular the problems around the geomagnetic equator are propagated into Swarm gravity field solutions when these kinematic orbit positions are used as pseudo-observations. The updates of the Swarm GPS receiver tracking loop settings in 2015 may have significantly improved the situation regarding ionosphere-induced artifacts (Dahle, Arnold and Jäggi, 2017). However, also the ionospheric activity has decreased markedly since then and it is not clear whether the current tracking loop settings are optimal also during times of higher ionospheric activity.

Especially to process Swarm GPS data from the time prior to the tracking loop updates, it is necessary to address the ionosphere-induced artifacts and to apply measures to mitigate them. A measure applied already for the GOCE GPS data processing (which suffered from similar problems, Jäggi et al. (2015)) is to discard all GPS data with the first time derivative of the geometry-free linear combination L_{gf} of the GPS carrier phase observations on the two frequencies exceeding a certain threshold. Jäggi et al. (2016) used a threshold of 2 cm/s (as opposed to 5 cm/s for GOCE) and showed that the ionosphere-induced artifacts in the Swarm GPS-derived gravity fields along the geomagnetic equator can be significantly reduced. However,

orbit validation by means of SLR showed that the applied GPS data screening degraded the Swarm reduced-dynamic and kinematic orbits.

Further methods to handle affected Swarm GPS data have therefore been tested. To analyze the impact of the different methods, monthly gravity field models for November 2014 (Swarm-A and Swarm-C) and June 2015 (Swarm-C) have been derived from kinematic orbits, which have been computed with the corresponding data screening or weighting strategy. In addition, the reduced-dynamic and kinematic orbits have been independently validated by SLR.

The kinematic positions were sampled to 10 s in all tests. The gravity fields have been solved up to degree and order 70, the static AIUB GRACE field AIUB-GRACE03S was introduced as a priori field also up to degree and order 70.

2.3.1 Scenarios

Table 2-1 shows the used IDs to label the different shown solutions. Apart from the solution *an*, which is based on the "old" strategy to discard all GPS data with dL_{gf}/dt exceeding a threshold, all other solutions have been derived by down-weighting the GPS data instead of discarding it. This turns out to be beneficial for the orbit quality, see below, while incurring no significant deterioration in the gravity field quality. Notice that the data has been heavily and constantly down-weighted once a pre-defined threshold was exceeded. Only for the ROTI-based strategy a dynamical down-weighting has been chosen as described in https://presentations.copernicus.org/EGU2015-10477_presentation.pdf.

<i>ID</i>	<i>Strategy</i>
ab	Original GPS data
an	Discarding data with $dL_{gf}/dt > 2 \text{ cm/s}$
ai	Down-weighting data with $dL_{gf}/dt > 2 \text{ cm/s}$
ak	Down-weighting data with $dL_{gf}^2/dt^2 > 0.025 \text{ cm/s}^2$
ar	Down-weighting data with $dL_{gf}^2/dt^2 > 0.025 \text{ cm/s}^2$ and $ \phi < 50^\circ$
ap	Down-weighting data based on ROTI

Table 2-1: Solution IDs for the shown monthly gravity fields. ϕ denotes the geographical latitude of the Swarm satellite.

2.3.2 Analysis of November 2014 data

2.3.2.1 Swarm-A

Figure 2-1 shows the geoid height differences of the six different monthly Swarm-A gravity fields in Tab. 2-1 for November 2014. All geoid height differences shown are w.r.t. AIUB-GRACE03S and are filtered with a 400 km Gauss filter. The solution based on the original GPS data (ab) shows the well-known very dominant artifacts along the geomagnetic equator. The artifact is reduced at varying degrees, in all other solutions.

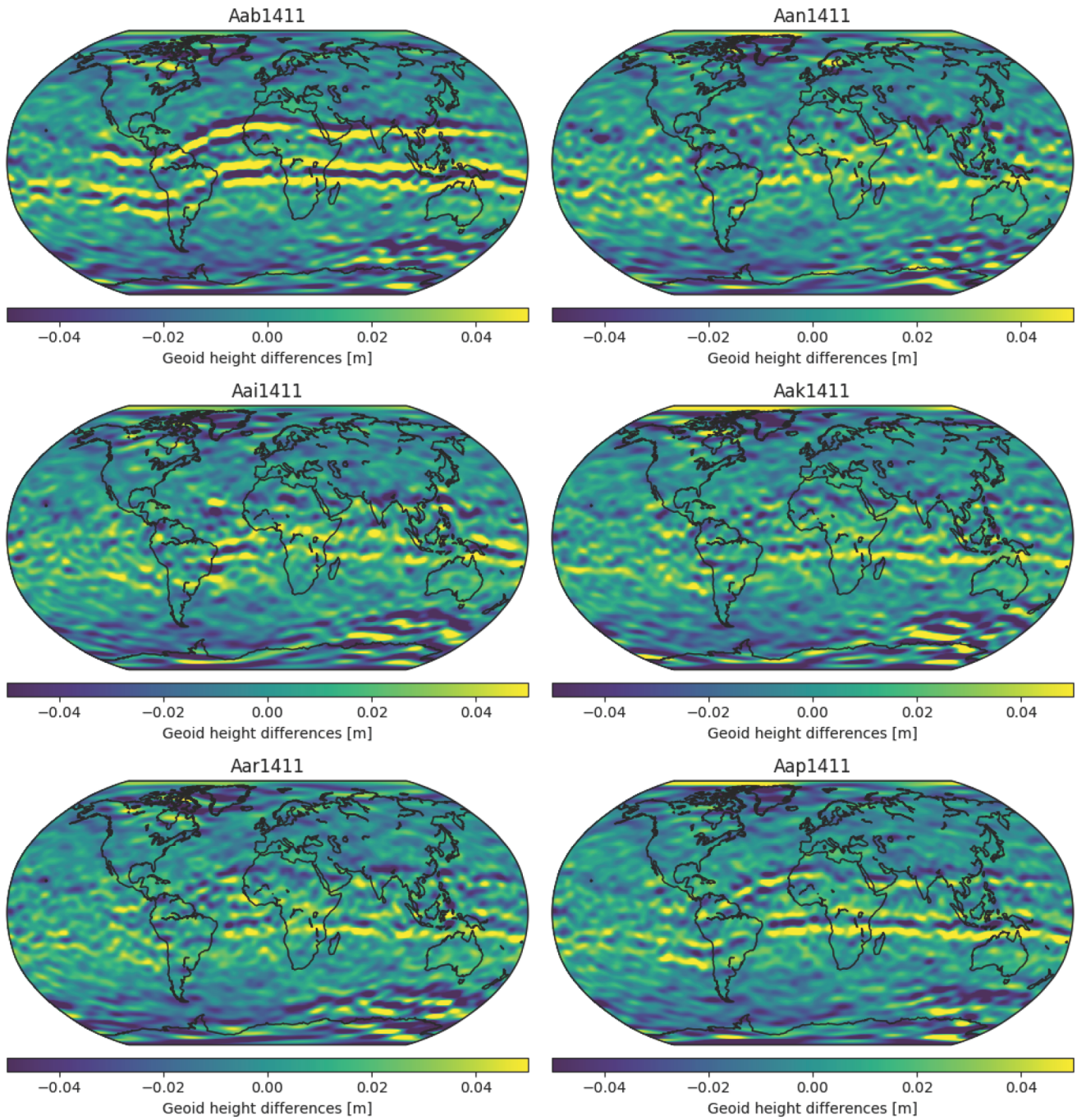


Figure 2-1 Geoid height differences of Swarm-A gravity fields for November 2014.

Figure 2-2 shows the difference and formal error degree amplitudes of the six gravity field solutions w.r.t. AIUB-GRACE03S.

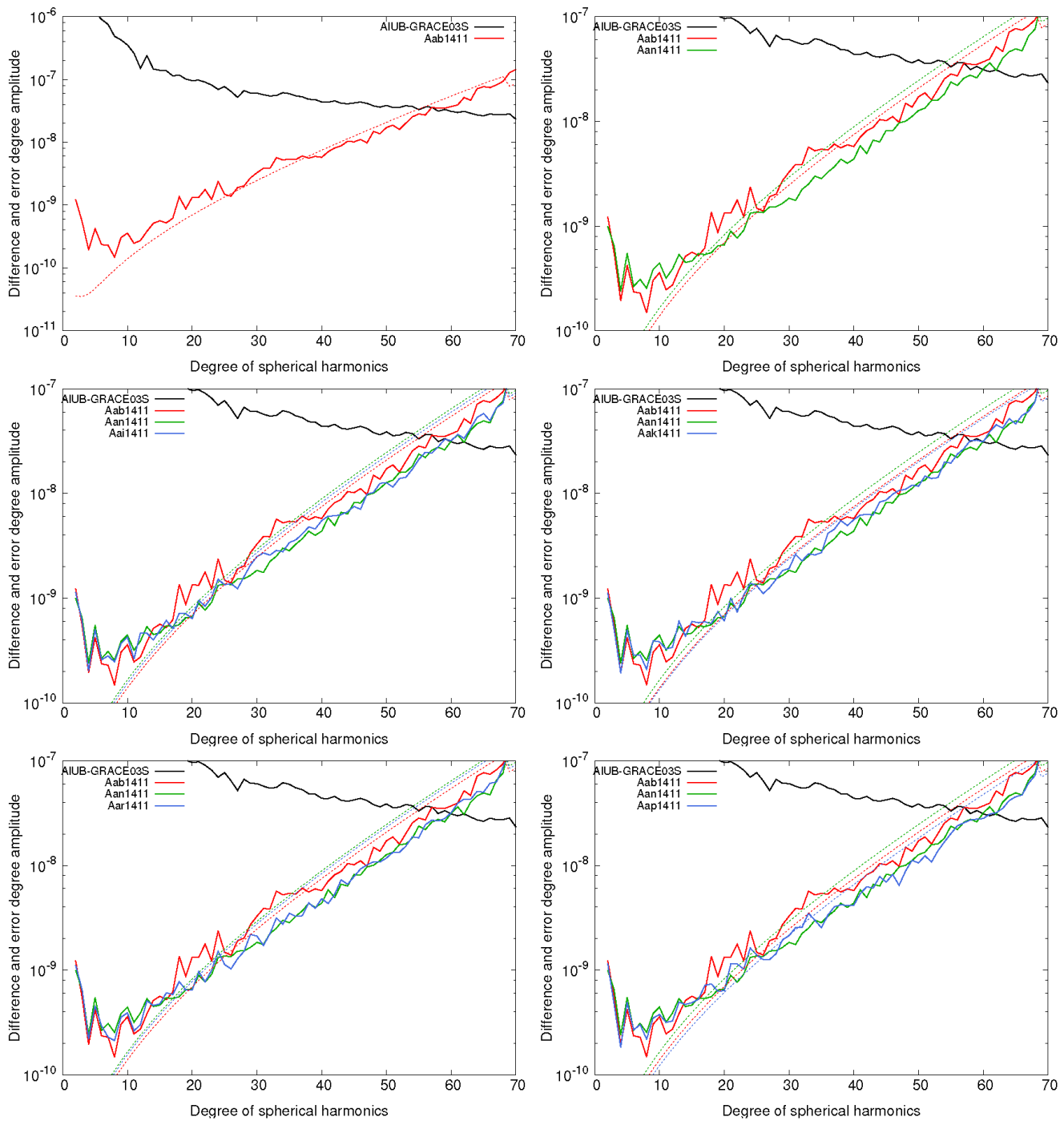


Figure 2-2 Difference and error degree amplitudes of Swarm-A gravity fields for November 2014.

Table 2-2 shows for all solutions the RMS values of the geoid height differences (bin-wise weighted with $\cos \phi$), as well as the weighted standard deviation of geoid height differences over the ocean. For the latter the field GOC05S has been subtracted and the fields have only been resolved to degree and order 40.

Multi-approach gravity field models from Swarm GPS data

SW_TN-02_ASU_GS_0001 version 1

2019-04-09

<i>ID</i>	<i>Wgt. geoid. ht. diff. RMS [mm]</i>	<i>Wgt. std. dev. over ocean [mm]</i>
ab	21.8	112.7
an	14.1	67.5
ai	15.2	74.2
ak	14.3	73.5
ar	14.2	69.3
ap	14.9	73.3

Table 2-2: Weighted geoid height difference RMS values and weighted standard deviations over the ocean for the different Swarm-A gravity field solutions for November 2014.

From Fig. 2-1 and Tab. 2-2, it can be seen that the screening applied so far (the *an* solution) is rather effective in removing the artifact around the geomagnetic equator. Figure 2-2 shows that the screening degrades the lowest degrees of the gravity field - a fact that has been reported already by Jäggi et al. (2016). The other weighting strategies also degrade the lowest degrees, however, in some cases (e.g. “an” and “ai”), clearly less.

Table 2-3 shows the mean values and standard deviations of SLR residuals for the reduced-dynamic and kinematic Swarm-A orbits. For the SLR validation, the station coordinates were introduced according to SLRF2014, no parameters have been estimated. The residuals of the following 12 stations were used to compute the statistics: Graz (7839), Greenbelt (7105), Haleakala (7119), Hartebeesthoek (7501), Herstmonceux (7840), Matera (7941), Mount Stromlo (7825), Potsdam (7841), Wettzell (SOSW, 7827), Wettzell (WLRS, 8834), Yarragadee (7090), and Zimmerwald (7810). The number of used SLR observations is 1150 for Swarm-A and November 2014.

<i>ID</i>	<i>Reduced-dynamic</i>		<i>Kinematic</i>	
	<i>Mean [mm]</i>	<i>Std. dev. [mm]</i>	<i>Mean [mm]</i>	<i>Std. dev [mm]</i>
ab	2.6	16.6	0.9	27.8
an	7.4	32.1	0.8	38.3
ai	0.3	22.1	5.9	39.5
ak	2.8	16.0	0.8	30.1
ar	2.8	18.1	0.6	31.8
ap	3.8	14.3	0.6	29.5

Table 2-3: Mean values and standard deviations of residuals for Swarm-A reduced-dynamic and kinematic orbits for November 2014.

The SLR validation reveals that the "old" screening (the *an* solution) significantly degrades the orbit quality, doubling and increasing by 37% the Std. relative to SLR measurements for the Reduced-dynamic orbit and KO, respectively. The degradation is smaller for the other strategies. Notice that, at least for the reduced-dynamic orbit, the SLR residuals for the orbits obtained by using the $dL_{gf}/dt > 2$ cm/s criterion for a down-weighting (*ai*) instead of an omission (*an*) are significantly smaller (the average discrepancy is reduced by a factor of 20). A very likely explanation for this is the larger number of carrier phase ambiguities which is set up during the data pre-processing when creating data gaps by discarding observations (not shown).

Multi-approach gravity field models from Swarm GPS data

SW_TN-02_ASU_GS_0001 version 1

2019-04-09

Page 13 of 44

The above results indicate that the weighting based on the 2nd derivative of $L_{gf}(ak)$ is the most promising one. It is capable of removing the artifacts around the geomagnetic equator about as efficient as the "old" approach, but does not degrade the orbits in terms of SLR residuals as much. Regarding the SLR validation, also the orbits obtained from a ROTI-based weighting (ap) are promising, but this approach does not seem to be as efficient in removing the artifact as the 2nd L_{gf} derivative.

2.3.2.2 Swarm-C

The same tests have been performed for the same month of November 2014 for Swarm-C. The conclusions drawn from the geoid height differences and difference degree amplitudes are basically identical and no plots are shown here. For completeness, however, Tab. 2-4 shows the weighted geoid height differences and the weighted standard deviations over the ocean for the Swarm-C November 2014 gravity fields, and Tab. 2-5 collects the SLR statistics of the corresponding orbits.

ID	Wgt. geoid. ht. diff. RMS [mm]	Wgt. std. dev. over ocean [mm]
ab	21.1	108.4
an	14.3	64.6
ai	14.6	67.0
ak	14.5	70.2
ar	13.8	64.2
ap	14.5	69.4

Table 2-4: Weighted geoid height difference RMS values and weighted standard deviations over the ocean for the different Swarm-C gravity field solutions for November 2014.

ID	Reduced-dynamic		Kinematic	
	Mean [mm]	Std. dev. [mm]	Mean [mm]	Std. dev [mm]
ab	4.6	15.9	1.0	26.7
an	5.6	25.0	3.1	38.1
ai	4.6	16.3	0.8	28.9
ak	4.8	16.0	0.6	31.3
ar	4.7	15.8	-0.1	28.3
ap	4.7	15.8	0.7	29.4

Table 2-5: Mean values and standard deviations of SLR residuals for Swarm-C reduced-dynamic and kinematic orbits for November 2014.

2.3.2.3 Preliminary conclusions

The tests in November 2014 suggest that the down-weighting based on the 2nd time derivative of L_{gf} seems to yield a promising compromise between reducing the ionosphere-induced artifacts and not degrading the orbits too much.

2.3.3 Analysis of June 2015 Swarm-A data

To analyze the screening and weighting strategies under different ionospheric conditions, the same tests have been performed for Swarm-A and June 2015. Figures 2-3 and 2-4 show the geoid height differences and the difference and error degree amplitudes of the resulting gravity field solutions. The corresponding RMS values of the geoid height differences, as well as the weighted standard deviations of geoid height differences over the ocean are shown in Tab. 2-6.

Multi-approach gravity field models from Swarm GPS data

SW_TN-02_ASU_GS_0001 version 1

2019-04-09

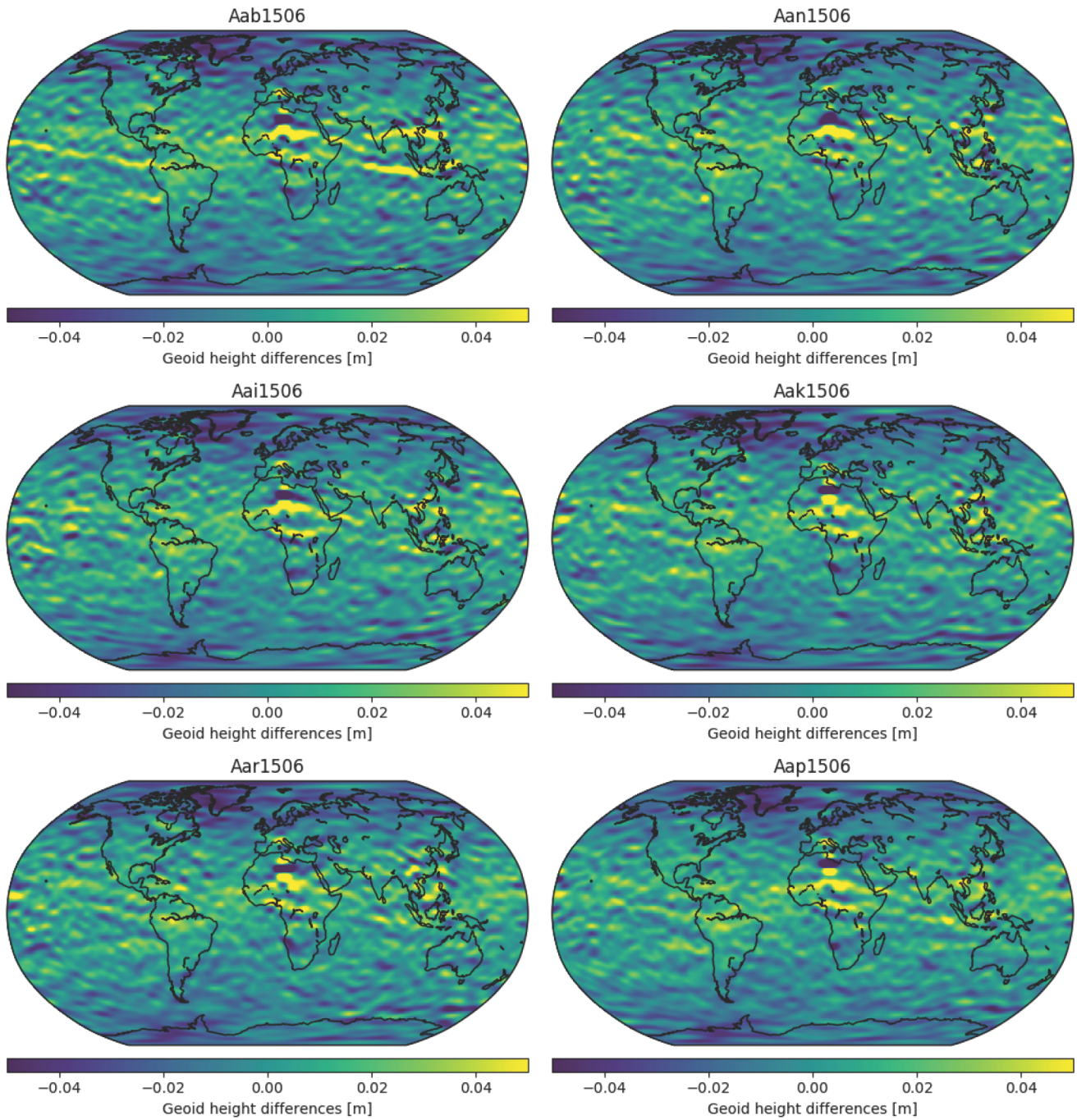


Figure 2-3 Geoid height differences of Swarm-A gravity fields for June 2015.

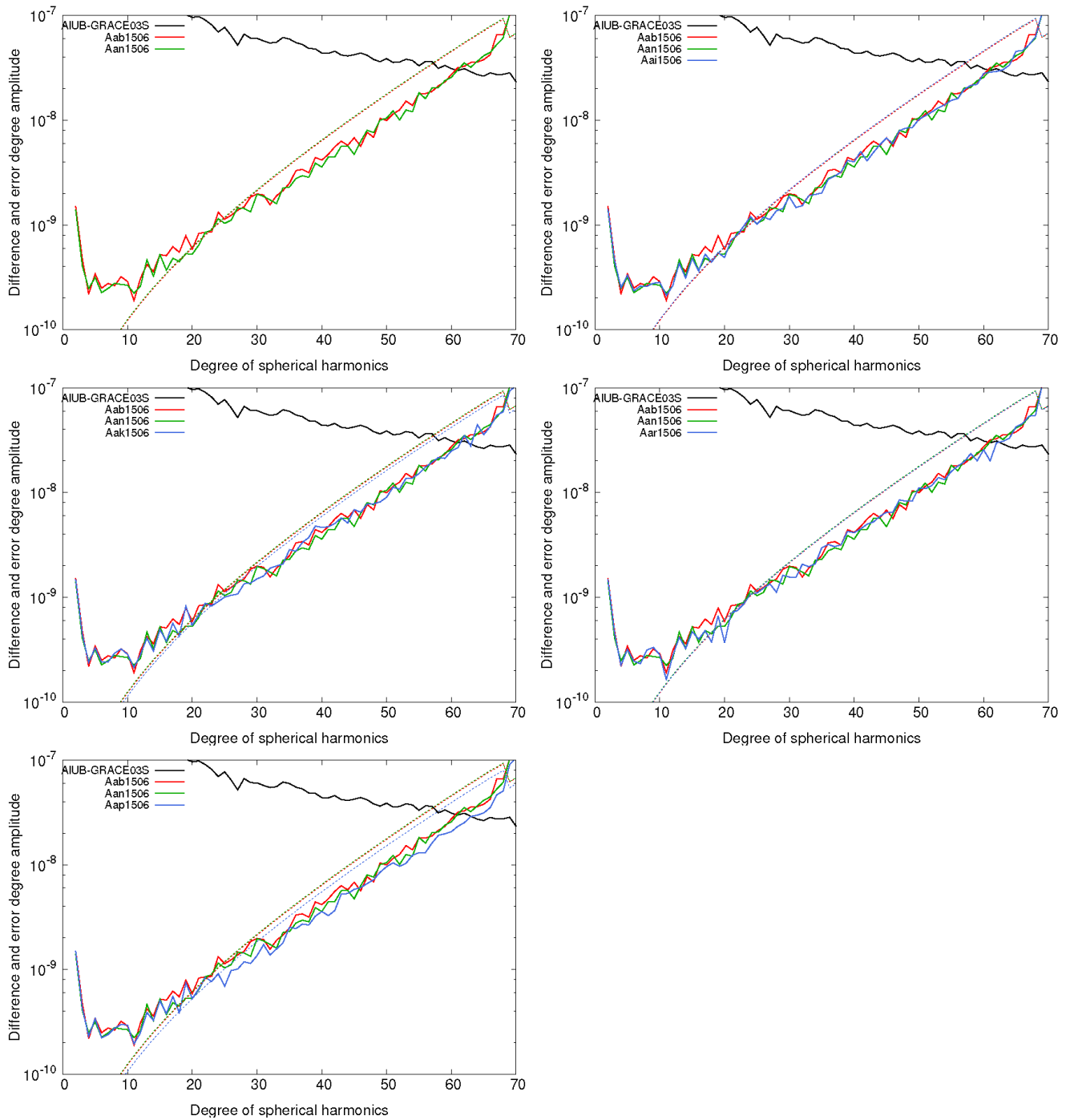


Figure 2-4 Difference and error degree amplitudes of Swarm-A gravity fields for June 2015.

<i>ID</i>	<i>Wgt. geoid. ht. diff. RMS [mm]</i>	<i>Wgt. std. dev. over ocean [mm]</i>
ab	14.3	55.3
an	13.0	53.6
ai	13.0	53.5
ak	13.3	51.3
ar	13.3	51.0
ap	12.2	44.6

Table 2-6: Weighted geoid height difference RMS values and weighted standard deviations over the ocean for the different Swarm-A gravity field solutions for June 2015.

Table 2-7 shows the SLR residual statistics for the reduced-dynamic and kinematic Swarm-A orbits of June 2015. In terms of these numbers the weighting strategies based on the 2nd time derivative of L_{gf} and based on ROTI perform well and comparably.

<i>ID</i>	<i>Reduced-dynamic</i>		<i>Kinematic</i>	
	<i>Mean [mm]</i>	<i>Std. dev. [mm]</i>	<i>Mean [mm]</i>	<i>Std. dev [mm]</i>
ab	3.5	15.6	2.8	17.3
an	3.6	15.6	1.8	16.2
ai	3.7	15.8	2.8	17.6
ak	3.6	15.7	2.7	17.4
ar	3.7	15.5	2.6	17.4
ap	3.3	15.5	2.7	17.1

Table 2-7: Mean values and standard deviations of residuals for Swarm-A reduced-dynamic and kinematic orbits for June 2015.

2.3.4 Summary

Compared to November 2014 the quality of the gravity fields is in general better and the strength of the ionospheric-induced artifact is generally reduced. While the solution based on the 2nd time derivative of L_{gf} performs well, the ROTI-based solution shows slightly smaller geoid height differences, noise over the ocean and difference degree amplitudes. It has to be noted that, in all cases, the ROTI-based GPS data screening leads to a slightly larger number of kinematic positions usable for the gravity field recovery.

2.4 Recommendations

Based on these findings, it can be recommended to apply a GPS data down-weighting strategy that is based on the 2nd time derivative of L_{gf} . Both for November 2014 and June 2015 this strategy proved efficient in removing the artifacts and in keeping a good orbit quality. Apparently, for months with lower ionospheric activity the ROTI-based approach is promising as well and, in the case of June 2015 leads to a slightly less noisy gravity field solution. Further tests over longer time spans might be needed to further investigate the impact of the two weighting strategies or of combinations thereof.

2.5 Acronyms

AIUB Astronomical Institute of the University of Bern, Switzerland,
www.aiub.unibe.ch

ASU	Astronomical Institute (Astronomický ústav), AVCR, www.asu.cas.cz/en
AVCR	Czech Academy of Sciences (Akademie věd České Republiky), Czech Republic, www.avcr.cz/en/
GPS	Global Positioning System
IfG	Institute of Geodesy Graz, TUG, www.itsg.tugraz.at
KO	Kinematic Orbit
MW	Melbourne-Wübbena
OSU	Ohio State University, www.osu.edu
POD	Precise Orbit Determination
ROTI	Rate of Total Electron Content (TEC) Index
SLR	Satellite Laser Ranging
SoW	Statement of Work, Doc. Ref. SW-SW-DTU-GS-111_ITT1-1
SNR	Signal-to-Noise Ratio
TEC	Total Electron Content
TU Delft	Delft University of Technology, www.tudelft.nl
TUG	Graz University of Technology, Austria, www.tugraz.at
WP	Work Package

2.6 Bibliography

- Condat, L. (2013). A Direct Algorithm for 1-D Total Variation Denoising. In: IEEE Signal Processing Letters 20.11, pp. 1054–1057. DOI: 10.1109/LSP.2013.2278339
- Dahle, C., D. Arnold and A. Jäggi (2017). Impact of tracking loop settings of the Swarm GPS receiver on gravity field recovery. In: Advances in Space Research 59.12, pp. 2843 –2854. DOI: <https://doi.org/10.1016/j.asr.2017.03.003>
- Ijssel, Jose van den et al. (2015). Precise science orbits for the Swarm satellite constellation. In: Advances in Space Research 56.6, pp. 1042 –1055. DOI: <https://doi.org/10.1016/j.asr.2015.06.002>
- Jäggi, Adrian et al. (2015). GOCE: assessment of GPS-only gravity field determination. In: Journal of Geodesy 89.1, pp. 33–48. DOI: 10.1007/s00190-014-0759-z

Multi-approach gravity field models from Swarm GPS data

SW_TN-02_ASU_GS_0001 version 1

2019-04-09

Page 18 of 44

Jäggi, A. et al. (2016). Swarm kinematic orbits and gravity fields from 18months of GPS data. In: Advances in Space Research 57.1, pp. 218 –233.

DOI: <https://doi.org/10.1016/j.asr.2015.10.035>

Pi, X. et al. (1997). Monitoring of global ionospheric irregularities using the Worldwide GPS Network. In: Geophysical Research Letters 24.18, pp. 2283–2286. DOI:

10.1029/97GL02273

3 WP221: Modeled non-gravitational accelerations (ASU)

Author(s): Ales Bezdek (WP221)

3.1 Introduction

The objective of WP221 is to produce the non-gravitational accelerations following the model implemented at ASU to be considered in WP220 (Section 6). According to the project proposal (TU Delft et al, 2017), the work to be carried out in this WP is:

1. Ensure that the in-house software is prepared to ingest Swarm Level 1B (L1B) data (KO and attitude);
2. Document the procedure used to produce the data;
3. Produce the time series of non-gravitational accelerations for the periods defined in WP220;
4. Exchange the data with WP220.

Point 1 had already been completed: the in-house ASU software produced many results using the Swarm L1B data, presented on Swarm Data Quality Workshops (2015–2017) and in publications (e.g., Bezděk et al., 2016, 2017; Encarnaç o et al., 2016).

This section addresses the remaining points.

3.2 Method

For processing the satellite orbital data, the coordinate transformations and the generation of modeled forces, on which the creation of the modeled non-gravitational accelerations of each Swarm satellite is based, the ASU home-made orbital propagator NUMINTSAT is used (Bezdek et al., 2009). In order to compute the non-gravitational forces, ESA provides scientific users with the physical properties of the satellite: its mass, cross-section in a specific direction, radiation properties of the satellite's surface and a macro model approximately characterizing the shape of the Swarm satellites. When representing the force due to atmospheric drag, we paid special attention to quantities usually having most uncertainty in their specific values. For neutral atmospheric density, we made use of the NRLMSISE-00 model. To have a realistic drag coefficient, for each satellite we estimated it by means of the long-term change in the orbital elements. The details of our approach can be found in references, e.g. (Bezdek, 2010; Bezdek et al., 2014, 2016, 2017).

3.3 Data – selected test months

In the selection of months, over which the analysis of WP220 will be carried out, the properties considered in the choice included:

- availability of the Swarm C accelerometer data recently released by ESA (see Section 5)
- availability of the GRACE gravity field monthly solutions as a reference
- ionospheric and geomagnetic activity
- accelerometer signal magnitude and variability
- geomagnetic activity.

Multi-approach gravity field models from Swarm GPS data

SW_TN-02_ASU_GS_0001 version 1

2019-04-09

Page 20 of 44

Based on e-mail discussions with the managers of WP220, WP222 and WP230, the following four months have been selected for a study on the usefulness of accelerometer (ACC) data vs. non-gravitational models (WP220):

- (A) High level of geomagnetic activity: Mar 2015
- (B) Higher level in ACC variability: Jan 2015 and Feb 2016
- (C) Lower level in ACC variability: Mar 2016

The selection of the test months was based among other things on the character of the non-gravitational accelerations for Swarm satellites in the period 19 July 2014 to 27 April 2016, for which the most update version of the official ESA calibrated ACC data is currently available (Swarm C, along track, 19 Jul 2014 to 27 Apr 2016, ACCxCAL_2 v. 0201). The properties of the selected months with respect to the above-cited criteria are given in Table 6-1.

<i>month and year</i>	<i>accelerometer variability</i>	<i>ionospheric activity</i>	<i>geomagnetic activity</i>	<i>accelerometer signal magnitude</i>
January 2015	high	high	low	high
February 2015	middle	middle	low	high
March 2015	low	high	high	high
January 2016	middle	low	low	low
February 2016	middle	low	low	low
March 2016	low	low	low	low

Table 3-1: List of months selected for the analysis in WP220.

All the partners in WPs 221, 222 and 223 have agreed with this selection and produced the necessary data. These include the modeled non-gravitational accelerations (WP221, WP222) and the measured accelerometer data from Swarm C (WP223).

3.4 Conclusions

All points of the WP221 task list have been fulfilled. Point 1 is discussed in Section 3-1, point 2 in Section 3-2. The modeled non-gravitational accelerations were provided for further use in WP220, thus completing points 3 and 4.

3.5 Bibliography

- Bezděk A, 2010. Calibration of accelerometers aboard GRACE satellites by comparison with POD-based nongravitational accelerations. *Journal of Geodynamics* 50(5), 410–423.
<http://dx.doi.org/10.1016/j.jog.2010.05.001>
- Bezděk A, Klokočník J, Kostelecký J, Floberghagen R, Gruber C, 2009. Simulation of free fall and resonances in the GOCE mission. *Journal of Geodynamics* 48(1), 47–53,
<http://dx.doi.org/10.1016/j.jog.2009.01.007>
- Bezděk A, Sebera J, Encarnação J, Klokočník J, 2016. Time-variable gravity fields derived from GPS tracking of Swarm. *Geophys. J. Int.* 205, 1665–1669.
<http://dx.doi.org/10.1093/gji/ggw094>

Multi-approach gravity field models from Swarm GPS data

SW_TN-02_ASU_GS_0001 version 1

2019-04-09

Page 21 of 44

- Bezděk A, Sebera J, Klokočník J, 2017. Validation of Swarm accelerometer data by modelled nongravitational forces. *Advances in Space Research* 59, 2512–2521. <http://dx.doi.org/10.1016/j.asr.2017.02.037>
- Bezděk A, Sebera J, Klokočník J, Kostelecký J, 2014. Gravity field models from kinematic orbits of CHAMP, GRACE and GOCE satellites. *Advances in Space Research* 53, 412–429. <http://dx.doi.org/10.1016/j.asr.2013.11.031>
- Encarnação J, Arnold D, Bezděk A, Dahle Ch, Doornbos E, van den IJssel J, Jäggi A, Mayer-Gürr T, Sebera J, Visser P, Zehentner N, 2016. Gravity field models derived from Swarm GPS data, 2016. *Earth, Planets and Space* 68:127. <http://dx.doi.org/10.1186/s40623-016-0499-9>
- TU Delft et al, 2017. Multi-approach gravity field models from Swarm GPS data – Proposal for Swarm DISC ITT 1.1.

4 WP222: Modeled non-gravitational accelerations (TU Delft)

Author(s): Eelco Doornbos (WP222)

4.1 Objective

The objective of WP222 is to produce the non-gravitational accelerations following the model implemented at TU Delft to be considered in WP220 (Section 6). The work to be carried out in this WP is:

1. Ensure that the in-house software is prepared to ingest Swarm L1B data (orbit and attitude);
2. Document the procedure used to produce the data;
3. Produce the time series of non-gravitational accelerations for the periods determined in WP220;
4. Exchange the data with WP220.

4.2 Method

For this work package, the existing Swarm processing software infrastructure, based on TU Delft's Near Real-Time Density Model (NRTDM) software, was employed. This software is used in the L1B to L2 processing in Delft, and therefore was already capable of ingesting the orbit and attitude data. A variety of models related to the non-gravitational forces is available in this software. In this case, the following selection was employed:

- Swarm panel model (macro model), based on geometry obtained from ESA and Astrium;
- Panel orientation based on Swarm quaternion data;
- Sentman's equations for satellite aerodynamics of single-sided flat panels, assuming diffuse reflection and energy flux accommodation set at 0.93;
- NRLMSISE-00 thermosphere model used for neutral density, as well as temperature and composition-dependence of Sentman's equations;
- Velocity of the atmosphere with respect to the spacecraft based on the orbit and attitude data, atmospheric co-rotation and modeled thermospheric wind using HWM07 and DWM07.
- Radiation pressure equations, taking into account absorption, diffuse reflection and specular reflection, according to optical properties of the surface materials supplied by ESA and Astrium;
- Solar radiation pressure based on the varying Sun-Satellite distance, and a conical Sun-Earth eclipse model taking into account atmospheric absorption and refraction (ANGARA implementation);
- Terrestrial radiation pressure, based on albedo and thermal IR radiation, based on ANGARA implementation, and monthly average albedo coefficients and IR irradiances from ERBE data;

The equations for the algorithms and references for these models are available in Doornbos (2012) with updates specific to Swarm provided by Siemes, et al. (2016).

The NRTDM software allows for exporting in the agreed-upon file format. The data for the period December 2013 until the end of January 2018, which include the test periods, was uploaded to the project server in monthly files.

4.3 Conclusions

All tasks of the WP221 task list have been fulfilled.

4.4 Bibliography

Doornbos, E. (2012). Thermospheric Density and Wind Determination from Satellite Dynamics. Springer Berlin Heidelberg. doi:10.1007/978-3-642-25129-0

Siemes, C., de Teixeira da Encarnação, J., Doornbos, E., van den IJssel, J., Kraus, J., Peřestý, R., et al. (2016). Swarm accelerometer data processing from raw accelerations to thermospheric neutral densities. *Earth, Planets and Space*, 68(1), 297. doi:10.1186/s40623-016-0474-5

5 WP223: Measured non-gravitational accelerations

Author(s): Ales Bezdek (WP223)

5.1 Introduction

The objective of WP223 is to prepare the measured non-gravitational accelerations of Swarm-C to be considered in WP220 (Section 6). According to the project proposal (TU Delft et al, 2017), the work to be carried out in this WP is:

1. Ensure the quality of the measured non-gravitational accelerations of Swarm-C for the periods defined in WP220 is adequate and conduct any necessary data screening;
2. Document the characteristics of the data and any screening procedures considered;
3. Prepare the time series of measured non-gravitational accelerations of Swarm-C to be ingested by the gravity field inversion software;
4. Investigate the quality of cross-track and radial accelerometer components of Swarm-C for their further use within this project; it is expected, however, that only along-track component of Swarm-C will be provided as the measured non-gravitational accelerations;
5. Exchange the data with WP220.

This section addresses all these points.

5.2 Methodology

Swarm accelerometer (ACC) data suffer from large temperature dependence (Swarm A/B, Swarm C less) and substantial ACC anomalies (steps, jumps, spikes, ...). The modeled non-gravitational accelerations look like a smoothed version of the accelerometer observations, but the accelerometer data generally supersede the modeled non-gravitational accelerations by providing more detailed information on high-frequency contents of the external perturbations. Information on the character of the accelerometer data from the three Swarm satellites is summarized in Bezděk et al. (2017).

5.2.1 Input accelerometer data

A large number of abrupt signal changes (steps, jumps etc.) makes it difficult to use the Swarm ACC data for science. For this reason ESA developed a step-correcting procedure, which has been applied to the Swarm C along-track ACC data (Siemes et al., 2016). This is the basic input data set used in this WP and provided to WP220 for further analyses. The step-corrected procedure was applied to the Level 1A (L1A) product ACCxSCI_1A and is provided by ESA as part of the most update version of the official calibrated ACC data product (Swarm C, along track, 19 Jul 2014 to 27 Apr 2016, ACCxCAL_2 v. 0201). For other ACC components, we made use of the L1A accelerometer data.

5.2.2 Calibration method

To reduce the high temperature dependence, we apply the method of *linear temperature correction*. First we demonstrated its good performance on reducing the temperature dependence of Swarm ACC data when compared to the physically modeled non-gravitational accelerations (Bezděk et al., 2017). There, the resulting plausible temperature-corrected Swarm ACC signal was based on using the modeled non-gravitational accelerations. The next step was to integrate the linear temperature correction into a calibration procedure for Swarm ACC data,

where the calibration standard is derived the KOs and gravity field models. The description of the calibration method, its good performance and first long-term results for the ACCxCAL_2 data set are provided in Bezděk et al. (2018). Here, the calibration method is applied to separate data blocks. To connect the values of the calibration parameters obtained in the blocks, we use Kalman filtering. The reason is that for each block we obtain point estimates of the calibration parameters, each time accompanied by the covariance matrix. The point estimates are usually highly correlated. Kalman filtering is an ideal tool to take into account a changing precision of the calibration parameters as well as their correlations. In this way we obtain an estimated set of calibration parameters for each epoch in the ACC data set.

5.3 Measured non-gravitational accelerations of Swarm-C

5.3.1 Along-track accelerometer component of Swarm-C

The results of applying the calibration procedure to step-corrected ACC data of Swarm-C for the periods defined in WP220 are in Figs. 5-1 to 5-4.

The adequacy of the proposed calibration method is validated by a comparison of the ASU calibrated ACC signal (blue) against physically modeled non-gravitational accelerations (green), which were computed independently (for details, see Section 3, WP221). Note the overall good match of the amplitude and long-term as well as short term variations of the two signals. The third signal shown in Figs. 5-1 to 5-4 is the ESA calibrated ACC signal provided in the ACCxCAL_2 product (red). This signal was derived using a different temperature correction (Siemes et al., 2016). Thus, a rather good match of the ASU and ESA calibrated ACC signals cross-validates both approaches.

As regards the data screening, only the evident gross outliers in the input step-corrected ACC data were replaced by interpolated values. The screening was done by excluding the points grossly outlying with respect to modeled non-gravitational accelerations.

Multi-approach gravity field models from Swarm GPS data

SW_TN-02_ASU_GS_0001 version 1

2019-04-09

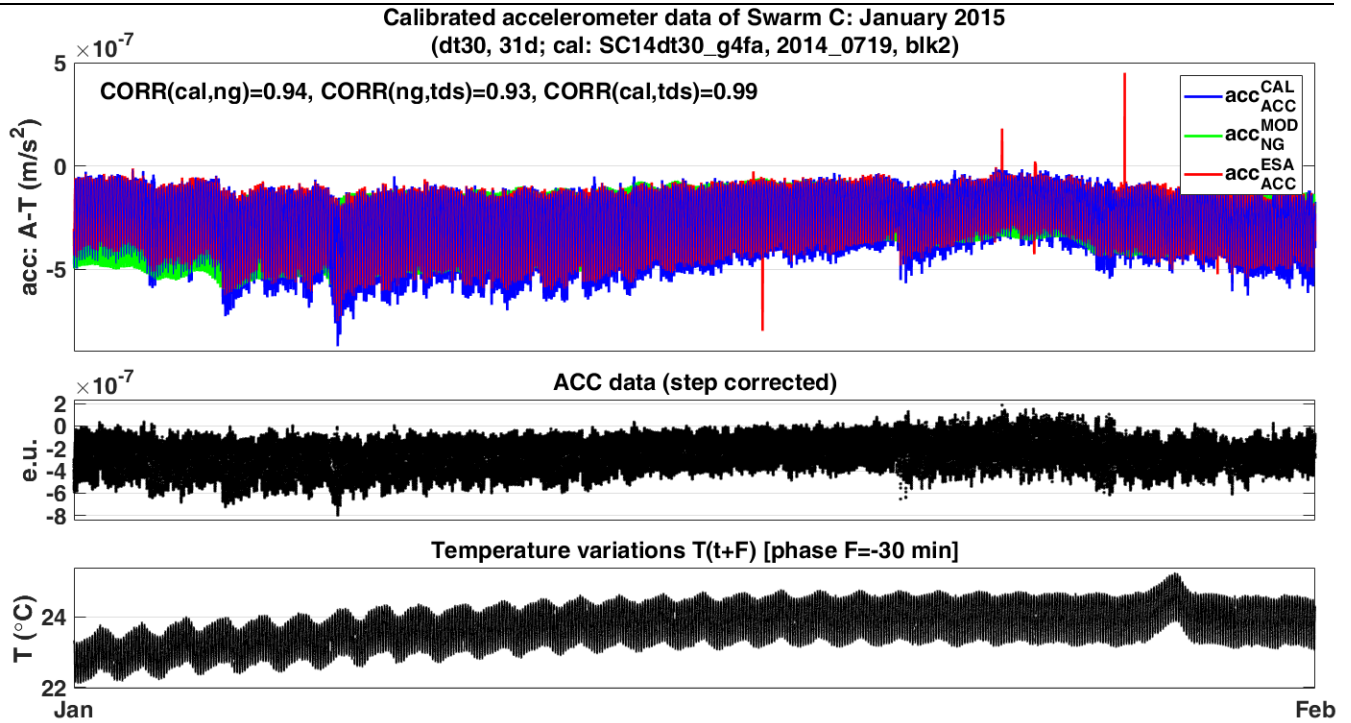


Figure 5-1 Calibrated accelerometer data, along-track component of Swarm C: January 2015.

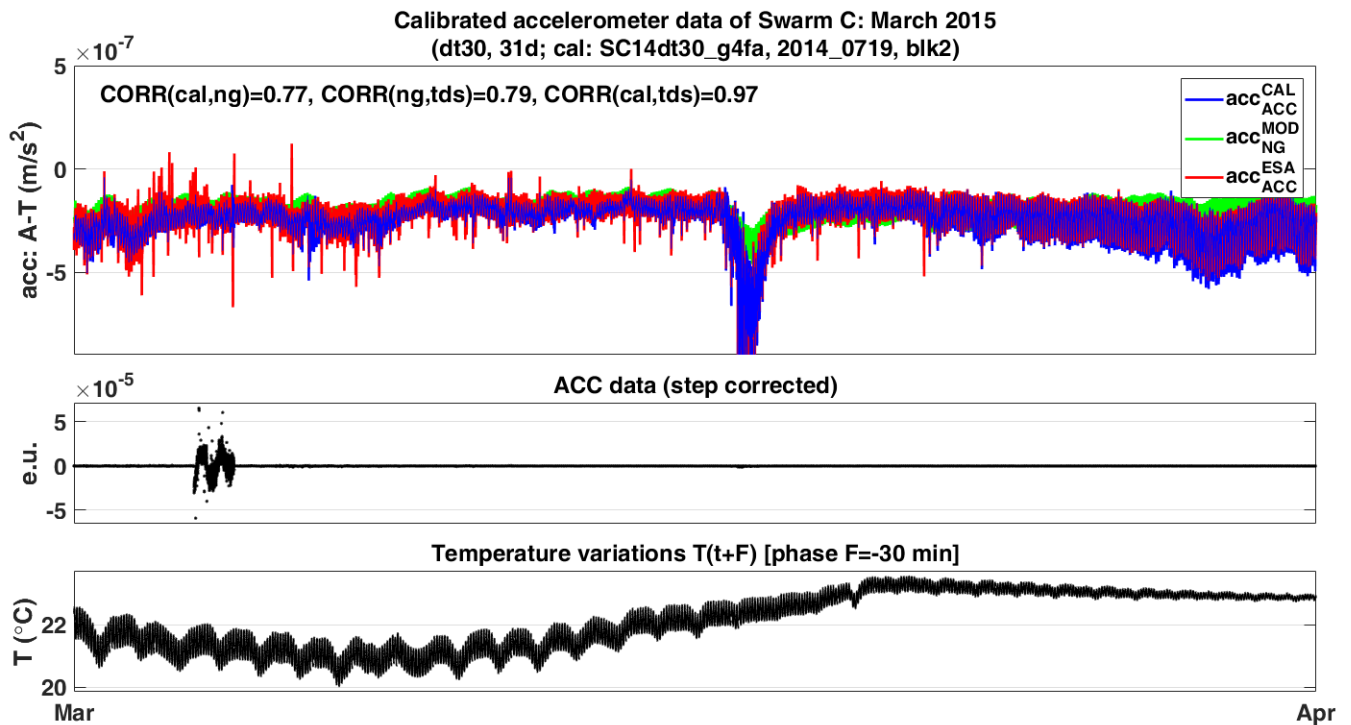


Figure 5-2 Calibrated accelerometer data, along-track component of Swarm C: March 2015.

Multi-approach gravity field models from Swarm GPS data

SW_TN-02_ASU_GS_0001 version 1

2019-04-09

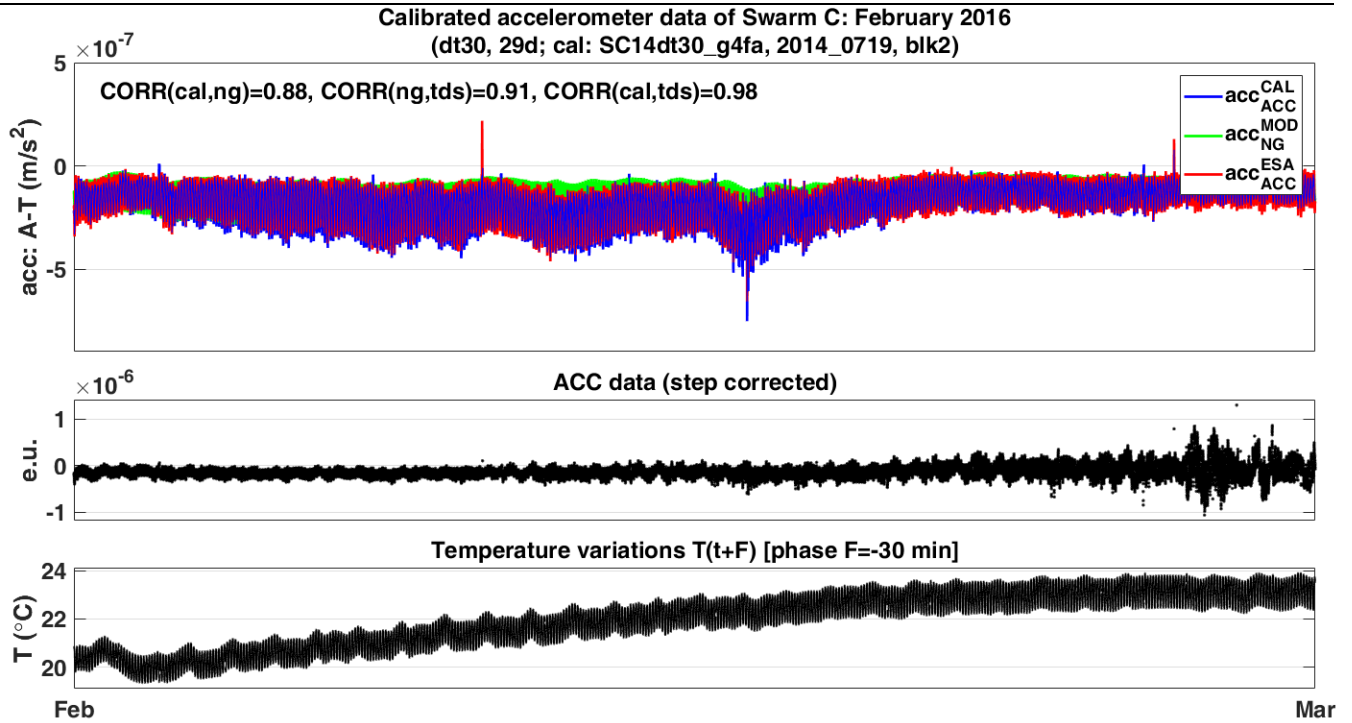


Figure 5-3 Calibrated accelerometer data, along-track component of Swarm C: February 2016.

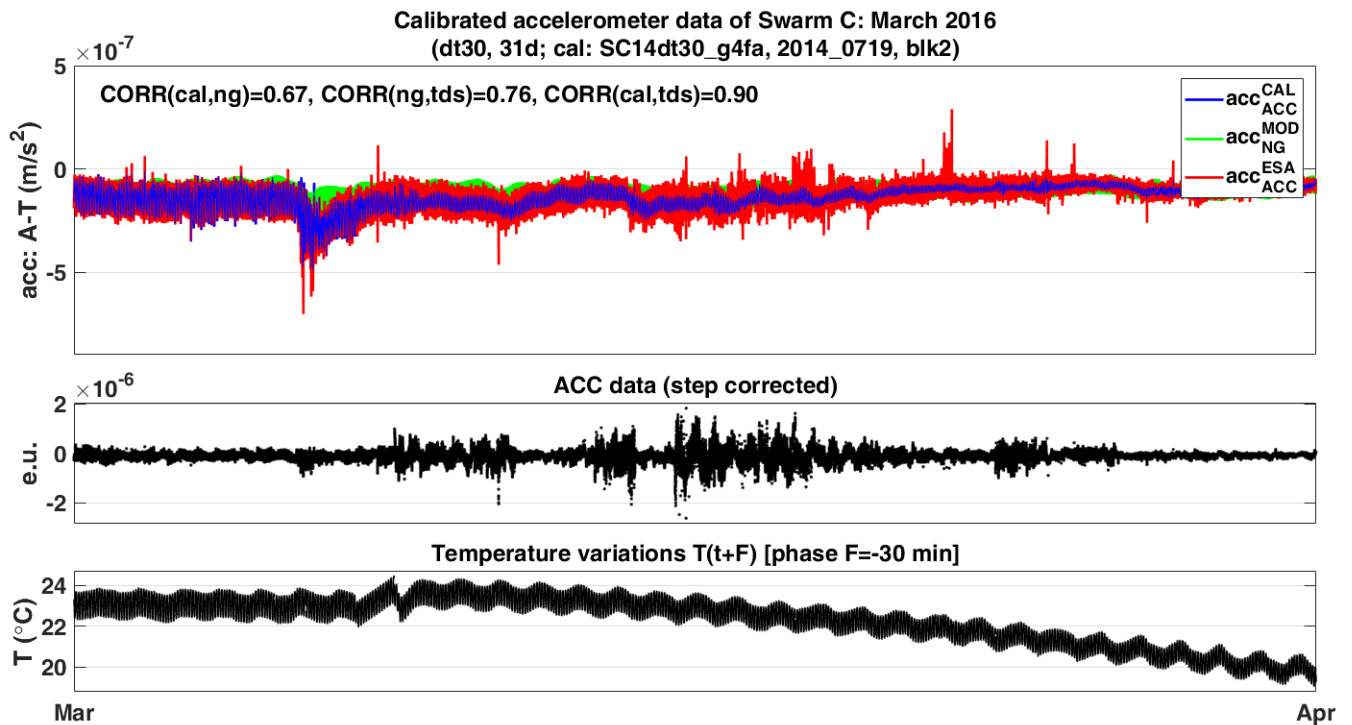


Figure 5-4 Calibrated accelerometer data, along-track component of Swarm C: March 2016.

5.3.2 Cross-track and radial accelerometer components of Swarm-C

To address point 4 in the WP task list, the same calibration method was applied to the cross-track and radial accelerometer components of Swarm-C.

In this case, as input data we used the raw L1A accelerometer data. Unfortunately, the ACC data components contain hardware-related anomalies, which for the along-track component are removed by the dedicated step-corrective procedure. Fig. 5-5 shows the disrupted data in all three ACC components of Swarm-C, Fig. 5-6 shows the step-corrected data for the along-track component. The cross-track and radial components of ACC data are left with the shown signal anomalies (Fig. 5-5 is typical). For further use in gravity field recovery, such anomalies have to be corrected in some way (step-corrective procedure or alike).

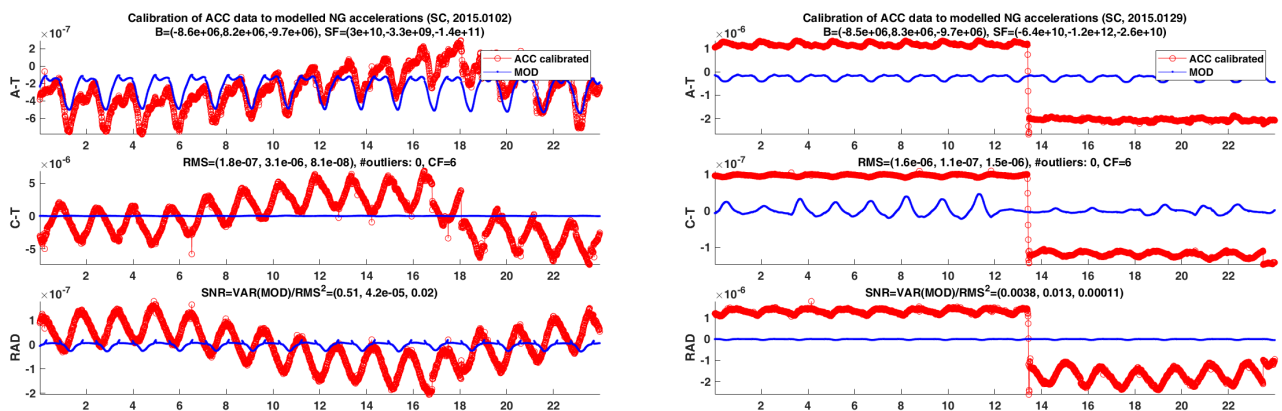


Figure 5-5 Comparison of Swarm-C accelerometer data to models. The panels show along-track (A-T), cross-track (C-T) and radial (RAD) components. Daily data for 2 Jan 2015 (on the left), 29 Jan 2015 (on the right).

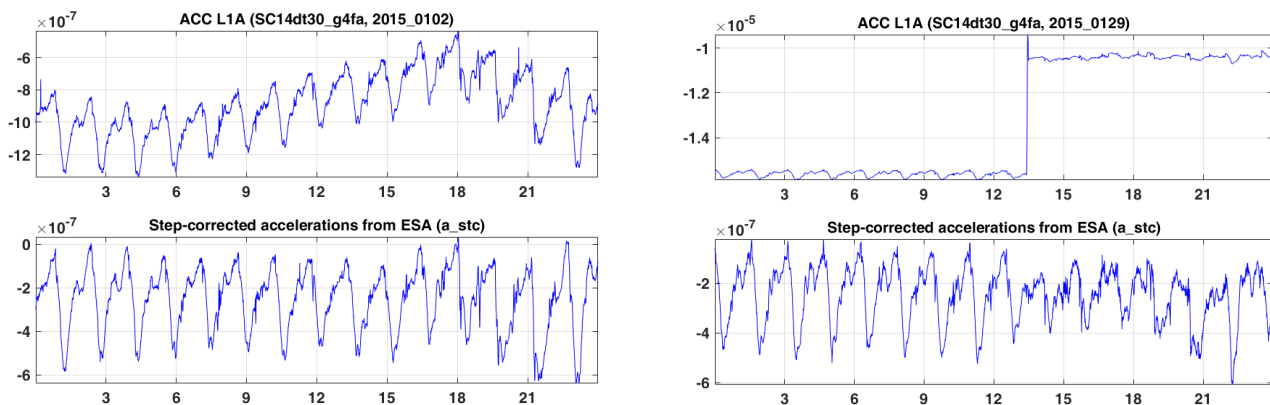


Figure 5-6 Step-corrective procedure applied to along-track component of Swarm-C accelerometer data shown in previous figure. Upper panel: raw L1A data. Lower panel: step-corrected data.

We applied the calibration procedure to cross-track and radial acceleration components, typical results for data blocks without anomalies are shown in Fig. 5-7. On the left, the ACC data in the cross-track component (blue) clearly contain the physical features due to the passage through the terminator and other influences as displayed by modeled non-gravitational accelerations (red). The correspondence might probably be improved by slightly shifting the temperature phase, but such fine-tuning is out of the scope of this research since it may change with the data

period. The mean uncertainty of the calibrated ACC curve is rather large, reaching 50% of the signal standard deviation, producing a not-optimum estimate of the trend. On the right panel of Fig. 5-7, the calibrated radial component (blue) does not correspond to the expected acceleration signal as shown by modeled non-gravitational accelerations (red). The main reason for such a bad calibration result is the noise in the calibration standard. The mean uncertainty is by 50% greater than the signal, so it is not possible to obtain reasonable values for the calibration parameters. These graphs are similar for LEO satellites. Similar results were obtained in simulations for the same orbital configuration of Swarm C and also for the ACC data of GRACE-A, with a similar ACC signal variability (24 Dec 2002). Even if one supposes that cross-track and radial ACC components were without hardware anomalies, due to a relatively large noise of the KO-based calibration standard, their positive impact on the gravity field recovery seems to be quite limited. Additionally, the same KO noise also enters the gravity field recovery itself, so most probably cross-track and radial ACC components do not have an important impact on the resulting fields, unless the KO noise would be substantially lower. On the other hand, we will show later that using the (step-corrected) *along-track* component of the Swarm-C ACC data in the gravity field recovery has a positive impact on the lowest degrees.

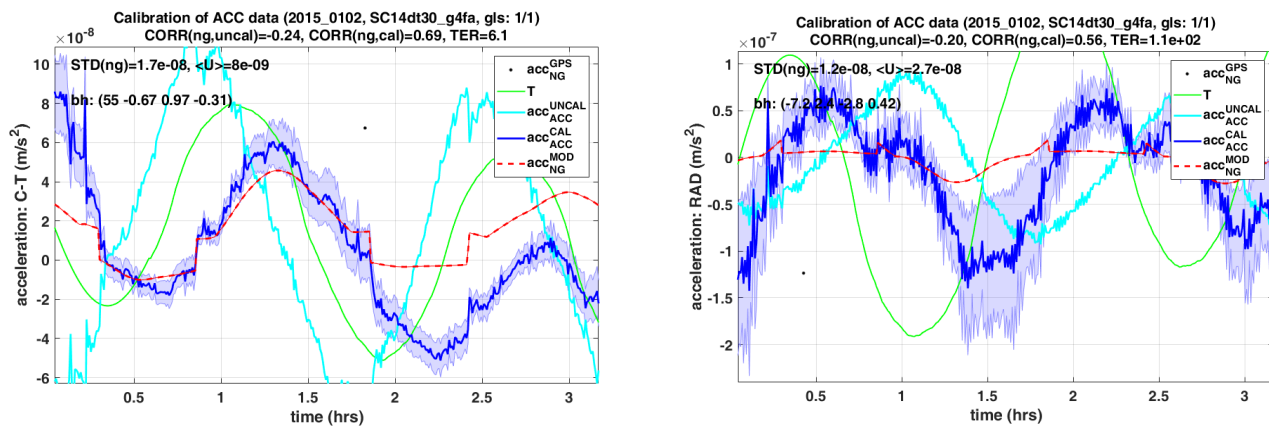


Figure 5-7 Calibration of cross-track (left) and radial (right) components of Swarm-C accelerometer data on 2 Jan 2015.

5.4 Conclusions

All points of the WP223 task list have been fulfilled. Points 1, 2 and 4 are discussed in Section 5-3. The calibrated along-track component of the Swarm-C accelerometer data was provided for further use in WP220 (Section 6), thus completing points 3 and 5.

5.5 Bibliography

Bezděk A, Sebera J, Klokočník J, 2017. Validation of Swarm accelerometer data by modelled nongravitational forces. *Advances in Space Research* 59, 2512–2521.
<http://dx.doi.org/10.1016/j.asr.2017.02.037>

Bezděk A, Sebera J, Klokočník J, 2018. Calibration of Swarm accelerometer data by GPS positioning and linear temperature correction. Under review in *Advances in Space Research*. Preprint:
http://www.asu.cas.cz/~bezdek/temp/Bezdek_2018_Calibration_Swarm_ACC_preprint.pdf

Multi-approach gravity field models from Swarm GPS data

SW_TN-02_ASU_GS_0001 version 1

2019-04-09

Page 30 of 44

Siemes C, Encarnação J, Doornbos E, van den IJssel J, Kraus J, Peřestý R, Grunwaldt L, Apelbaum G, Flury J, Olsen P.E., 2016. Swarm accelerometer data processing from raw accelerations to thermospheric neutral densities. *Earth Planets Space* 68, 92.

<http://dx.doi.org/10.1186/s40623-016-0474-5>.

TU Delft et al, 2017. Multi-approach gravity field models from Swarm GPS data – Proposal for Swarm DISC ITT 1.1.

6 WP220: Trade-off between Swarm accelerometer data and non-gravitational models

Author(s): Ales Bezdek (WP220)

6.1 Introduction

The objective of WP220 is to address Task 2 of the SoW, specifically the items referring to the non-gravitational accelerations used in the inversion of the gravity fields. To meet this objective, the Decorrelated Acceleration Approach (DAA), implemented at ASU, will be used to compute 3 types of gravity fields, each considering:

- a) the non-gravitational model of ASU (WP221),
- b) the non-gravitational model of TU Delft (WP222) and
- c) the accelerometer measurements from Swarm-C and the non-gravitational model of ASU for the other two satellites (WP223).

Therefore, the activities of this WP consist of the following points:

1. Selecting a small number of months, in which the analysis is to be performed;
2. Coordinating with WP221, WP222 and WP223 the production of non-gravitational accelerations, their format, upload to the exchange server and remaining details deemed important;
3. Performing preliminary validation of the three types of non-gravitational accelerations;
4. Producing three types of gravity field models considering each of the types of non-gravitational accelerations listed above;
5. Analyzing and interpreting the residual relative to GRACE;
6. Documenting the findings.

The selection of which months will be analyzed should be sufficient to describe different levels of geomagnetic activity and consider the (expected) quality of the corresponding GRACE solution.

This section addresses all these points. It uses the results provided by the preceding WPs, described in their specific sections, namely WP221 (Sec. 3), WP222 (Sec. 4) and WP223 (Sec. 5).

6.2 The Decorrelated Acceleration Approach

The Decorrelated Acceleration Approach (DAA) connects the double-differentiated GPS positions to the external forces acting on the satellite (Bezděk et al. 2014). This approach computes the geopotential harmonic coefficients from a linear (not linearized) system of equations. The observations are first transformed to the inertial reference frame before differentiation to avoid the computation of fictitious accelerations. The differentiation of noisy observations leads to the amplification of the high-frequency noise. However, it is possible to handle the high-frequency noise with a decorrelation procedure, so far for this purpose a fitted autoregressive process has been used. The DAA method has been developed by the ASU and applied successfully to Swarm KOs to produce the monthly gravity fields (Bezděk et al., 2016).

6.3 Results

6.3.1 Preliminary validation of the three types of non-gravitational accelerations

The validation and inter-comparison of the three types of non-gravitational accelerations a)–c) listed in Section 6.1 has been done and presented several times (e.g. Bezděk et al., 2018). Also Figures 5-1 to 5-4 in Section 5 (WP223) demonstrate a good correspondence between the three acceleration signals. We consider this cross-checking of the signals both for the absolute value as well as for the long-term and short-term variability to be a sufficient preliminary validation for our purposes.

6.3.2 Comparison of gravity fields using accelerometer data vs. non-gravitational models

6.3.2.1 Degree difference amplitudes for January 2015

The upper left panel of Fig. 6-1 compares the three gravity field solutions for Swarm-C derived from its GPS positions in January 2015. In the along-track component, the use was made of the ASU non-gravitational model (NG ASU; green), the TU Delft non-gravitational model (NG TUD; blue) and the calibrated accelerometer data (ACC; red). The degree difference amplitudes show clearly that using the ACC data improved the lowest degrees of the obtained Swarm-C monthly gravity solution. This is in accordance with the fact that using accelerometer data is beneficial for lowest degrees also in the standard GRACE gravity field recovery (e.g. Klinger and Mayer-Gürr, 2016). In Fig. 6-1 as a reference we used the GOCO05s model including its time-variable components (Mayer-Gürr et al., 2015), the GRACE KBR monthly field provided similar results; this agrees with our findings presented later in this section showing a good correspondence between the differences of our GPS fields compared to GOCO05s or to monthly KBR fields.

It is known that the signal from the on-board accelerometers of Swarm satellites suffers from anomalies. So far ESA has released only the along-track accelerometer component of Swarm-C. The next step in obtaining the Swarm gravity monthlies is to combine the solutions of all three Swarm satellites. The results for January 2015 are shown in the remaining three panels of Fig. 6-1. The upper right panel shows the separate solutions for Swarm A/B/C and their combination (in black), when as non-gravitational input we used uniquely the ASU models (NG ASU). In the lowest degrees, the performance of all three Swarm solutions is comparable. The same conclusion can be drawn for the solutions in the lower left panel, where in the inversion the Swarm-C along-track non-gravitational component was given by the TUD model. Finally, the lower right panel of Fig. 6-1 provides evidence that using accelerometer data produced a visibly better Swarm-C field and subsequently increased its weight in the combined solution at the lowest degrees.

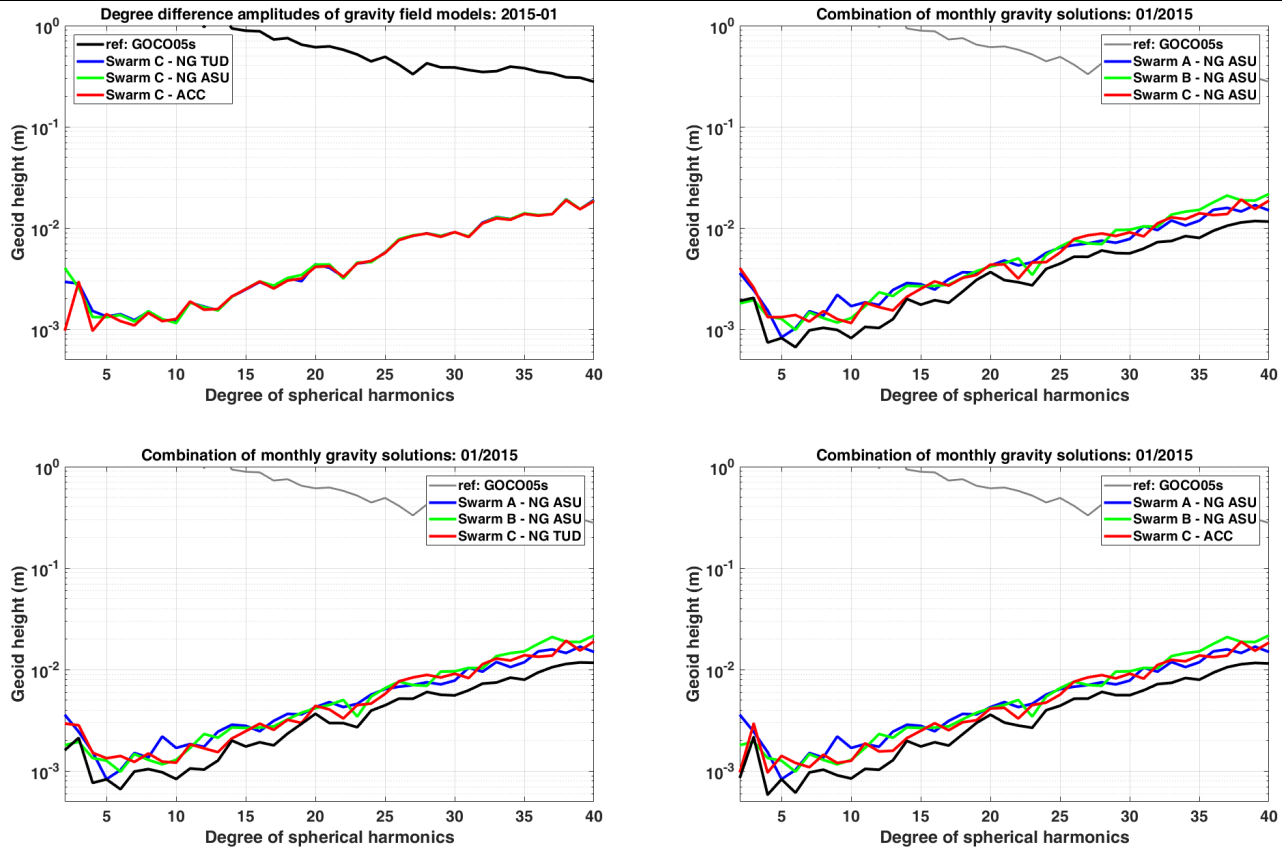


Figure 6-1 Degree difference amplitudes showing a positive impact of including ACC data for the monthly gravity field in Jan 2015. Upper left: Comparison of Swarm C gravity fields using NG TUD/NG ASU/ACC accelerations. Upper right: Combination of the Swarm A/B/C fields (thick black) using NG ASU in the Swarm C solution. Lower left: Ditto for NG TUD. Lower right: Ditto for ACC data.

6.3.2.2 Reference: GRACE monthly gravity fields

To be able to compare the quality of the Swarm GPS-based gravity fields with the standard GRACE monthly gravity fields derived from KBR measurements, it would be advantageous to have an indicator as a single number. For this purpose, we chose the difference in the geoid height on a regular grid between Swarm GPS fields and the reference, which is represented by the ITSG-Grace2016 monthly solutions (Mayer-Gürr et al., 2016). We note that similar results were obtained using the GRACE monthly solutions computed by UT CSR. The resulting differences are shown in the left-hand part of Tab. 6-2. For Jan 2015, the first line shows that indeed the ACC-based Swarm field is closer to the reference (numbers in green) compared to the monthlies using the non-gravitational models. (The difference between this combined Swarm A+B+C field and the GRACE monthly field for Jan 2015 is shown in the upper left panel of Fig. 6-2.) The results shown in the left-hand part of Tab. 6-2 indicate that using ACC data for the computation of Swarm GPS fields improved their correspondence to the monthly KBR reference in the three 2015 test months, whereas no improvement was achieved for the three test months in 2016. Looking at the characteristics listed in Tab. 6-1, this implies better results are obtained using the ACC data, when the magnitude of the accelerometer signal is larger.

Multi-approach gravity field models from Swarm GPS data

SW_TN-02_ASU_GS_0001 version 1

2019-04-09

	KBR (ITSG-GRACE2016)			GOCO05S		
	NG ASU	NG TUD	ACC	NG ASU	NG TUD	ACC
1/2015	16.2	15.6	15.0	16.7	16.5	15.9
2/2015	18.8	18.0	17.9	18.0	17.7	17.5
3/2015	16.4	16.5	16.1	16.2	16.3	16.0
1/2016	20.3	20.0	20.5	17.5	17.3	17.3
2/2016	23.9	22.3	25.6	15.2	14.3	16.3
3/2016	17.1	15.6	18.5	12.5	12.4	12.9

Table 6-1: Geoid height differences [mm] on a 1°×1° grid for different combined Swarm A+B+C solutions with respect to the corresponding reference fields (left: ITSG-Grace2016; right: GOCO05s). Applied 500-km Gaussian filtering. We defined the difference as $D = \sqrt{MED^2 + (3 \cdot MAD)^2}$, where MED is median, MAD is median absolute deviation, D is computed over grid points having their latitude $|\phi| < 85^\circ$. This is simply a more robust analogy to the usual RMS value.

6.3.2.3 Reference: GOCO05s model

The six test months were selected from those, for which we had a step-free ACC signal, computed by a dedicated procedure by ESA (Jul 2014 to Apr 2016). Another important point is the availability of GRACE KBR fields used as a standard, against which the Swarm GPS fields were tested. To be able to decide in the future, whether for a month in question one should use the non-gravitational accelerations given by the calibrated ACC data (as in Jan–Mar 2015), or rather given by the non-gravitational models (as in Jan–Mar 2016), we need to find a reference not derived from the actual GRACE measurements. We tested several global time-varying gravity field models, and it was the GOCO05s model, which produced the results agreeing most satisfactorily with those based on the GRACE KBR monthlies. The right-hand part of Tab. 6-2 shows the differences of the Swarm fields relative to the GOCO05s model values. The conclusions implied by KBR and those implied by GOCO05s are compatible, except for Jan 2016, when GOCO05s indicates the same quality of the ACC-based and model-based GPS fields. This case can be resolved by defining that in the gravity field recovery the use will be made of ACC data, only when the GOCO05s difference of such an ACC-based gravity field is lower compared to the field based on non-gravitational models.

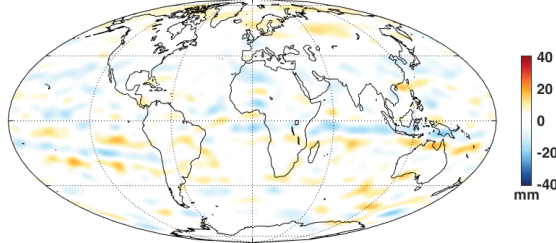
Fig. 6-2 shows several example maps of the geoid height differences. For months Jan 2015, Mar 2015 and Mar 2016, in the left-hand column there are the differences with respect to the KBR monthly fields, while in the right-hand column their counterparts computed using GOCO05s.

Multi-approach gravity field models from Swarm GPS data

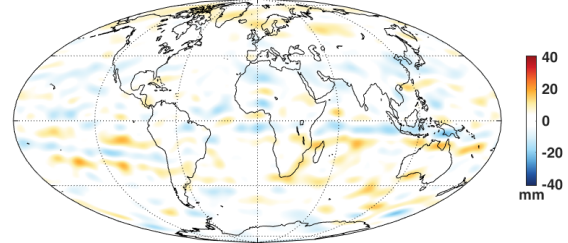
SW_TN-02_ASU_GS_0001 version 1

2019-04-09

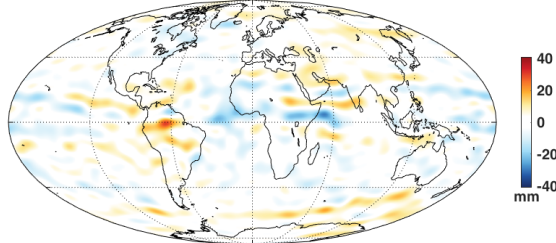
Difference: $n_{max}=40$ (~500 km), GF: 500 km, med/mad: 0.5 ± 15.0 mm (15.0 mm)
"Swarm A+B+C (2015_01, ACC)" vs "itsg16_2015_01"



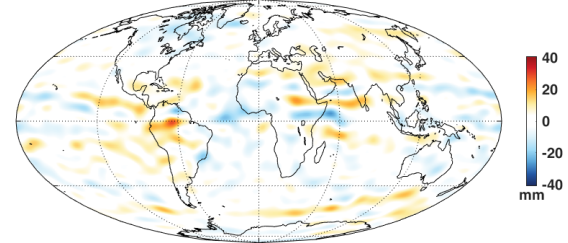
Difference: $n_{max}=40$ (~500 km), GF: 500 km, med/mad: 0.3 ± 15.9 mm (15.9 mm)
"Swarm A+B+C (2015_01, ACC)" vs "GOCO05s"



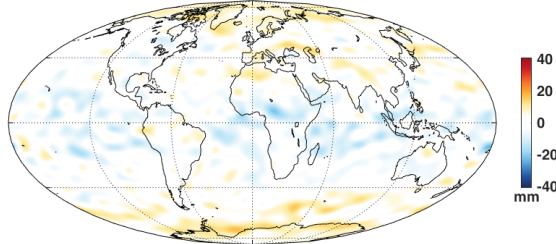
Difference: $n_{max}=40$ (~500 km), GF: 500 km, med/mad: 0.9 ± 16.1 mm (16.1 mm)
"Swarm A+B+C (2015_03, ACC)" vs "itsg16_2015_03"



Difference: $n_{max}=40$ (~500 km), GF: 500 km, med/mad: -0.2 ± 16.0 mm (16.0 mm)
"Swarm A+B+C (2015_03, ACC)" vs "GOCO05s"



Difference: $n_{max}=40$ (~500 km), GF: 500 km, med/mad: 1.9 ± 18.4 mm (18.5 mm)
"Swarm A+B+C (2016_03, ACC)" vs "itsg16_2016_03"



Difference: $n_{max}=40$ (~500 km), GF: 500 km, med/mad: 0.7 ± 12.8 mm (12.9 mm)
"Swarm A+B+C (2016_03, ACC)" vs "GOCO05s"

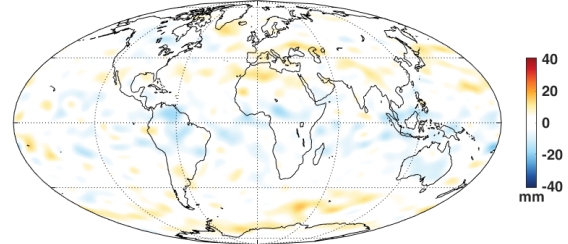


Figure 6-2 Geoid height differences between the combined Swarm A+B+C gravity field and the corresponding ITSG-Grace2016 fields (left column) and GOCO05s (right column) for monthly solutions January 2015, March 2015 and March 2016 (from top to bottom). The shown Swarm fields used the ACC data as the non-gravitational signal.

6.4 Conclusions

WP220 addressed the question related to the Swarm GPS-derived gravity field computation, whether in such a computation it is better to use the non-gravitational accelerations measured by the onboard accelerometer compared to using non-gravitational models. Currently, the only available step-corrected accelerometer data set is the along-track component of the accelerometer aboard Swarm-C. For the comparison, two sets of modeled non-gravitational accelerations were computed by ASU and TUD. The analysis was carried out over six months in 2015 and 2016, for which both the step-corrected accelerometer data as well as the reference GRACE monthly gravity fields were available.

The results are described in the left-hand part of Tab. 6-2. In summary, the Swarm monthly gravity fields computed using the ACC data performed better in January–March 2015, which is indicated by lower differences relative to the corresponding GRACE monthly solutions (green numbers). On the other hand, over January–March 2016, the ACC-based Swarm gravity fields were not better compared to the gravity fields computed using the non-gravitational models (red

numbers). In the second case, better results (lower values) were obtained by non-gravitational models computed by TUD.

The worse performance of ACC data in this later 2016 period may be related to the decreasing level of solar activity, which is approaching the minimum of its 11-year cycle, expected to be reached around 2019. Through the atmospheric density and ensuing air drag, the low level of solar activity has a direct impact on the accelerometer measurements. The nearer to the solar cycle minimum, the lower magnitude and variability of the accelerometer signal is. Another related factor might be a worse performance of the accelerometer calibration procedure under low levels of solar activity, resulting from the lower signal-to-noise ratio.

For the test periods, we used the GRACE gravity fields derived from the GRACE KBR data observed over the months in question. Within this WP, we also tried to find a means to be able to possibly distinguish the months of better accelerometer performance in the periods, when no GRACE monthly fields are available (after June 2017). It has turned out that this is possible by using the time-variable model GOC005s as a reference (the right-hand part of Tab. 6-2).

6.4.1 Suggested approach

Following these results, we suggest a similar analysis to be performed for every available current and future monthly Swarm GPS data set. Namely to compute the three types of the Swarm gravity fields, as the data in the along-track non-gravitational component of Swarm-C using ACC/NG ASU/NG TUD data respectively; finally to compare these three solutions to the time-variable GOC005s model. In case that no ACC data set is available, the use can be made only of the two non-gravitational models. Based on the assessment, the finalized non-gravitational data set is to be compiled which will use either the accelerometer data or the data coming from one of the modeled data sets, whichever produces the best results. This whole procedure – gravity field recovery, computing the test statistic and final compilation of the recommended non-gravitational data set – can be automated. The automated procedure will produce control figures to display the results for a possible quick check.

6.4.1.1 *Necessary prerequisite: step-corrected ACC data provided by ESA*

As for the accelerometer data, this suggested approach relies on the availability of the step-corrected accelerometer data, which has been produced by ESA for selected time periods using a dedicated software tool (Siemes et al., 2016). This tool performs a semi-automatic step correction and needs a manual intervention of an operator. Due to the fact that the currently available along-track accelerometer component of Swarm-C is of better quality compared to other Swarm accelerometer data, we believe that it is sufficient to provide only this component. The step-corrected accelerometer data is a necessity, otherwise the numerous hardware-related signal anomalies spoil the gravity field recovery. We note that the production of this step-corrected accelerometer has been done by ESA and as such it is external with respect to this DISC project consortium.

6.4.1.2 *Supporting reasons to continue the Swarm accelerometer data processing*

There are two reasons why to expect an increasing percentage of months, where the Swarm accelerometer data will outperform the non-gravitational models in the gravity field recovery:

1. The so-called 11-year solar cycle is near its minimum; the actual cycle length varies between 10–11.5 years, the last minimum ended late in 2009. The early start of the new cycle will increase air drag and thus the signal measured by the Swarm onboard accelerometers.
2. In the years to come, the Swarm satellites will decay and progressively lose their altitude, which will cause an increase in the acting non-gravitational forces. Therefore, the magnitude of the signal measured by the Swarm accelerometers will gradually increase as well and this way also its measurement characteristics like the signal-to-noise ratio will improve.

6.5 Bibliography

- Bezděk A, Sebera J, Encarnação J, Klokočník J, 2016. Time-variable gravity fields derived from GPS tracking of Swarm. *Geophys. J. Int.* 205, 1665–1669.
<http://dx.doi.org/10.1093/gji/ggw094>
- Bezděk A, Sebera J, Klokočník J, Kostelecký J, 2014. Gravity field models from kinematic orbits of CHAMP, GRACE and GOCE satellites. *Advances in Space Research* 53, 412–429.
<http://dx.doi.org/10.1016/j.asr.2013.11.031>
- Bezděk A, Sebera J, Klokočník J, 2018. Calibration of Swarm accelerometer data by GPS positioning and linear temperature correction. Under review in *Advances in Space Research*. Preprint:
http://www.asu.cas.cz/~bezdek/temp/Bezdek_2018_Calibration_Swarm_ACC_preprint.pdf
- Klinger B, Mayer-Gürr T, 2016. The role of accelerometer data calibration within GRACE gravity field recovery: Results from ITSG-Grace2016. *Advances in Space Research* 58, 1597–1609.
<http://dx.doi.org/10.1016/j.asr.2016.08.007>
- Mayer-Gürr, Torsten; Behzadpour, Saniya; Ellmer, Matthias; Kvas, Andreas; Klinger, Beate; Zehentner, Norbert (2016): ITSG-Grace2016 - Monthly and Daily Gravity Field Solutions from GRACE. GFZ Data Services. <http://doi.org/10.5880/icgem.2016.007>
- Mayer-Gürr, T., Rieser, D., Zehentner, N., Kvas, A., Klinger, B., Pail, R., Gruber, T., Fecher, T., Rexer, M., Schuh, W.-D., Kusche, J., Brockmann, J.-M., Baur, O., Hoeck, E., Krauss, S., Jaeggi, A., 2015. The combined satellite gravity field model GOCO05s. Presented at: EGU General Assembly 2015, Vienna, Austria, *Geophysical Research Abstracts*, vol. 17. EGU2015-12364.
<http://www.goco.eu>
- Siemes C, Encarnação J, Doornbos E, van den IJssel J, Kraus J, Peřestý R, Grunwaldt L, Apelbaum G, Flury J, Olsen P.E., 2016. Swarm accelerometer data processing from raw accelerations to thermospheric neutral densities. *Earth Planets Space* 68, 92.
<http://dx.doi.org/10.1186/s40623-016-0474-5>
- TU Delft et al, 2017. Multi-approach gravity field models from Swarm GPS data – Proposal for Swarm DISC ITT 1.1.

7 WP230: Kinematic baselines for gravity field estimation

Author(s): Norbert Zehentner (WP230), Adrian Jäggi (WP231), Xinyuan Mao (WP232)

7.1 Introduction

7.1.1 WP230: KBs for gravity field estimation

The main objective of this work package was to investigate a possible added value of Kinematic Baselines (KBs) for gravity field estimation. The basic assumption for this investigation is the fact that by using relative positioning methods to determine the baseline between two LEO satellites it might be possible to achieve higher relative accuracies and thus also improve to gravity field inversion. The purpose of WP230 was to provide an analysis of the effect on the final gravity field results and subsequently give some guidelines for future studies or projects.

7.2 Methodology

7.2.1 WP232: Kinematic baselines produced at TU Delft

This research is accomplished by using a GPS High Precision Orbit Determination Software Tools (GHOST) add-on tool called Multiple Orbit Determination using Kalman filtering (MODK). GHOST is a precise orbit determination software package developed by The German Space Operations Center (GSOC) with support from TU Delft.

MODK includes both a forward and backward filter and iterates until convergence. The EKF first runs from the first epoch to the last epoch of each 24-hours orbit arc with 5 second step. For each epoch, the covariance matrix of the estimated parameters is recorded. The estimated float integer ambiguities and the corresponding covariance matrices are used by the Least-squares Ambiguity De-correlation Adjustment (LAMBDA) algorithm in order to fix the maximum number of integer ambiguities (subset approach). The EKF smooths both solutions according to the bi-directional covariance matrices recorded at each epoch. In the next iteration, the smoothed orbit and fixed ambiguities are set as input and it is attempted to fix more ambiguities. Iterations are repeated until no new integer ambiguities are fixed.

After the convergence of the reduced-dynamic baseline, a KB solution is produced as well using the least squares method. To this aim, the same frequency-dependent GPS observations and fixed integer ambiguities on the two frequencies are used, where one satellite (Swarm-A) is kept fixed at the reduced-dynamic Precise Baseline Determination (PBD) solution. At least 5 observations are required on each frequency to form good geometry. To minimize the influence of wrongly fixed ambiguities and residual outliers, a threshold of 2-sigma of the carrier phase residual standard deviation statistics is set, which results in eliminating around 5% data. A further screening of 3 cm is set to the Root-Mean-Square statistics of the kinematic PBD carrier phase observation residual. It is able to screen out the solutions influenced by large wrongly fixed ambiguities and bad phase observations. The kinematic PBD also runs bi-directional and two solutions are averaged according to the epoch-wise covariance matrices from the least squares method.

Multi-approach gravity field models from Swarm GPS data

SW_TN-02_ASU_GS_0001 version 1

2019-04-09

Page 39 of 44

Seven months data is processed in this research, January 2015, March 2015, January 2016, February 2016, March 2016, June 2016, July 2016 and August 2016. A few days (15 January 2015, 19 March 2015, 3 March 2016, 16 June 2016 and 25 August 2016) are excluded due to large satellite maneuvers. For the 2015 data, the baseline consistency between kinematic and reduced-dynamic solutions is at a level of 1-3 cm in each individual direction (radial/along-track/cross-track). The ionospheric activity level has been decreasing since the early 2015. Moreover a few modifications and a new GPS RINEX converter have been made to the Swarm on-board GPS receivers between 2015 and 2016. These are proved to be effective to improve the PBD solution. After all the changes, this research eventually (June-August, 2016) shows a kinematic to reduced-dynamic baseline consistency level of sub-cm in each individual direction, with more than 95% available kinematic baselines for each day. The external Satellite Laser Ranging (SLR) validation confirms that the reduced-dynamic orbit precision obtained in this study reaches a level of 2 cm, which is comparable with the official European Space Agency (ESA) orbit solutions. This solution might provide insightful information for the gravity field recovery.

7.2.2 WP231: Kinematic baselines produced at AIUB

This research is accomplished by using the Bernese GNSS Software (BSW). BSW is a software package developed at AIUB for high-precision analysis of GNSS data.

Kinematic and reduced-dynamic baselines are determined according to the procedures previously described by (Jäggi et al., 2007, 2012). The positions of one satellite (Swarm-A) are kept fixed to a reduced-dynamic solution generated from zero-difference (ZD) ionosphere-free GPS carrier phase observations. Reduced-dynamic orbit parameters of the other satellite (Swarm-C) are then estimated by processing double-difference (DD) ionosphere-free GPS carrier phase observations with DD ambiguities resolved to their integer values. First, the Melbourne-Wübbena linear combination is analyzed to resolve the wide-lane ambiguities, which are subsequently introduced as known to resolve the narrow-lane ambiguities together with the reduced-dynamic baseline determination. For the kinematic baseline determination the same procedure may be used, but it turned out to be more robust to introduce the resolved ambiguities from the previously performed reduced-dynamic baseline determination and not to make an attempt to independently fix carrier phase ambiguities in the KB determination. Exactly the same carrier phase ambiguities are therefore fixed in both, the reduced-dynamic and the kinematic baseline determination.

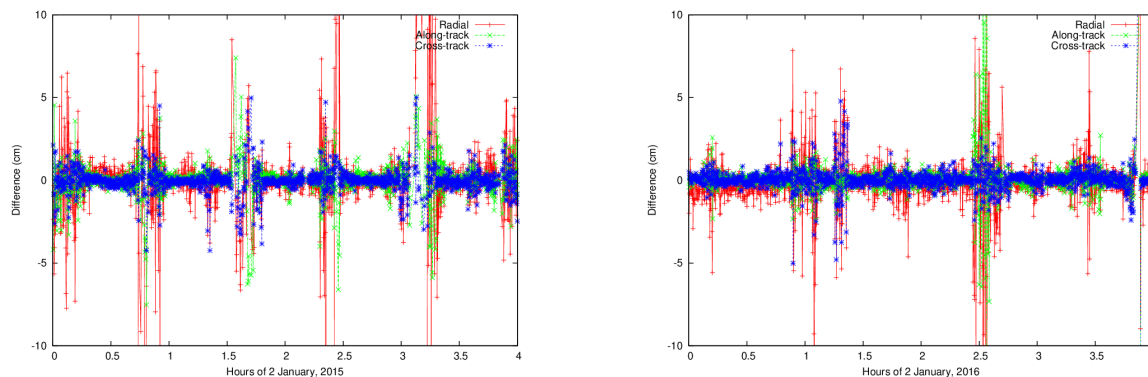


Figure 7-1 Differences between reduced-dynamic ambiguity-fixed and kinematic ambiguity-fixed baseline components for the first four hours of an example day in 2015 (left) and 2016 (right).

Figure 7-1 shows for two example days in 2015 and 2016 the differences between the reduced-dynamic ambiguity-fixed and kinematic ambiguity-fixed baseline components. The differences do not show the once-per-revolution-like signatures typically observed in orbit comparisons as a result of the successful fixing of the carrier phase ambiguities. Due to the decreasing ionospheric activity and the changes made to the Swarm on-board GPS receivers between 2015 and 2016, the baseline consistency is less degraded by large deviations over the polar regions for the 2016 solutions. Especially in summer 2016 the overall daily standard deviations may be as low as 10-15mm, 4-6mm, 3-5mm on average for the radial, along-track, cross-track directions, respectively. It should be noted, however, that daily standard deviations are always dominated by the low quality kinematic positions over the polar regions. When focusing on “unproblematic periods”, e.g., the first good period of 2015 shown in Fig. 7-1, standard deviations of 3.8 mm, 2.4mm, and 2.2mm may be observed for 2015. The corresponding results for the first good period of 2016 shown in Fig. 7-1 are 5.1mm, 2.1mm, and 2.8mm for 2016. The “inner precision” of the Swarm GPS data is thus of a very good quality, probably even slightly better before the tracking loop updates have been performed as it would be expected.

7.2.3 Gravity field inversion from kinematic baselines and orbits

The inversion of gravity field results from kinematic orbits and baselines was carried out at the IfG. The variational equations approach (VEA, Montenbruck and Gill, 2000) implemented at the IfG was used to compute two different solutions for each of the KBs, provided by TUD and AIUB. The VEA and its application to KOs and inter-satellite KBs corresponds to the processing scheme used for the production of the ITSG-Grace2016 (Mayer-Gürr et al., 2016).

First step was to select a few suitable test months with varying data quality. The main criteria for the selection have been:

- Grace monthly solutions are available for validation purposes
- Months with “good” GPS data quality are included as well as months with “bad” data quality
- Some months should overlap with the test months selected in WP220 for the accelerometer data tests

The descriptions “good” and “bad” data quality refer to several issues in the context of Swarm GPS data. “Good” means that an error found in the RINEX converter is solved (fixed since 12. April 2016), the settings of the receiver tracking loop bandwidths are optimized (several changes during lifetime), and the ionospheric activity is at a low level. In contrast to that “bad” data should be a time period for which these issues are not solved and the ionospheric activity is high. In total we have selected 7 test months.

- January and March 2015: “bad” quality months
- February and March 2016: “intermediate” months
- June-August 2016: “good” months

The kinematic baselines computed within WP231 and WP232 have been exchanged between the project partners in the newly defined sp3k format (TN-01), which is closely related to the

existing sp3c format but including an additional digit after the comma to ensure sufficient precision.

To enable Swarm baseline processing in the existing software for the VEA at the IfG and follow the processing scheme adopted for the generation of the ITSG-Grace releases, the kinematic baselines have been converted to GRACE-like range and range-rate observations. These derived observations are introduced into the gravity inversion process as if they were collected by the K-Band ranging instrument. Investigations have shown that either ranges or range-rates introduced as observations produce the same results. For our tests we have used ranges, as the kinematic baselines in fact represent range observations and not range-rates. The introduction of the full 3D information of the GPS baselines is not possible with the current software and implementing this functionality is not within the scope of this project. In addition to the baseline observations, KOs are also needed in the gravity field inversion process. They are routinely produced by TUD as well as AIUB and uploaded to the project server. The baseline solution of a particular institute has been combined with the corresponding kinematic orbit of the same institute. Data sampling used for all tests was 10 seconds for the kinematic baselines as well as the kinematic orbits.

In total 4 different solutions have been computed:

1. hl SST from TUD kinematic orbits
2. ll+hl SST from TUD kinematic orbits and baselines
3. hl SST from AIUB kinematic orbits
4. ll+hl SST from AIUB kinematic orbits and baselines

All of these four solutions have been produced for all 7 test months with a maximum degree and order of 60.

7.3 Results

As already mentioned in the previous section, we have computed a set of four different solutions for each of the 7 test months. Figure 7-2 to 7-3 show difference degree amplitudes with respect to the static part of the gravity field model GOCO05S (Mayer-Gürr et al., 2015) in terms of geoid heights. For comparison the corresponding month from the ITSG-Grace2016 (Mayer-Gürr et al., 2016) time series is also shown. For all months it can be seen that the solutions are slightly different. There are small differences between the two institutes as well as between the hl-only and the ll-hl solutions. Differences are larger for those months with "bad" data quality, whereas for months with "good" data quality all four solutions are almost identical. In months with "bad" data quality the ll+hl solution experiences degradation in higher degrees with respect to the hl solution. This issue would need some further investigations to find the cause.

“bad” data quality months

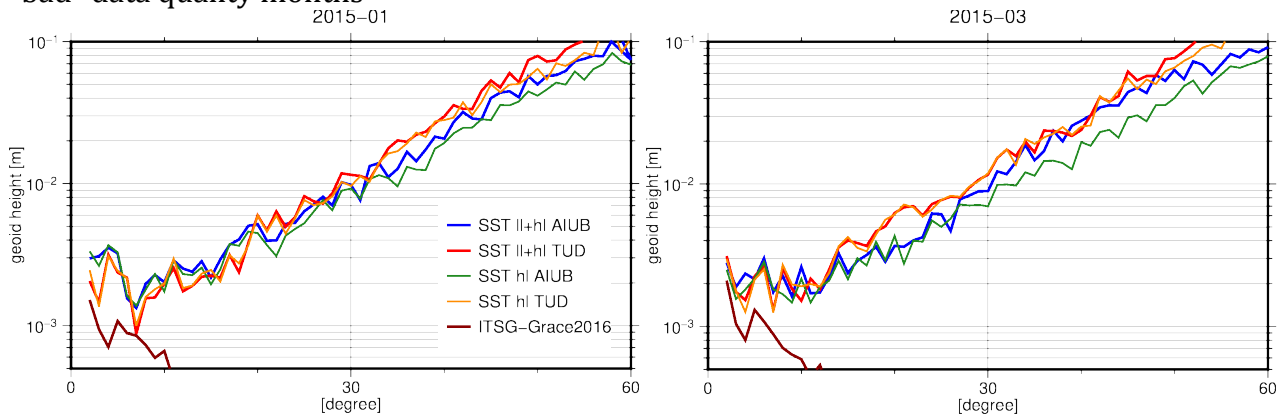


Figure 7-2: Difference degree amplitudes of all four test solutions for “bad” data quality test months with respect to GOCO05S (Mayer-Gürr et al., 2015).

“intermediate” data quality months

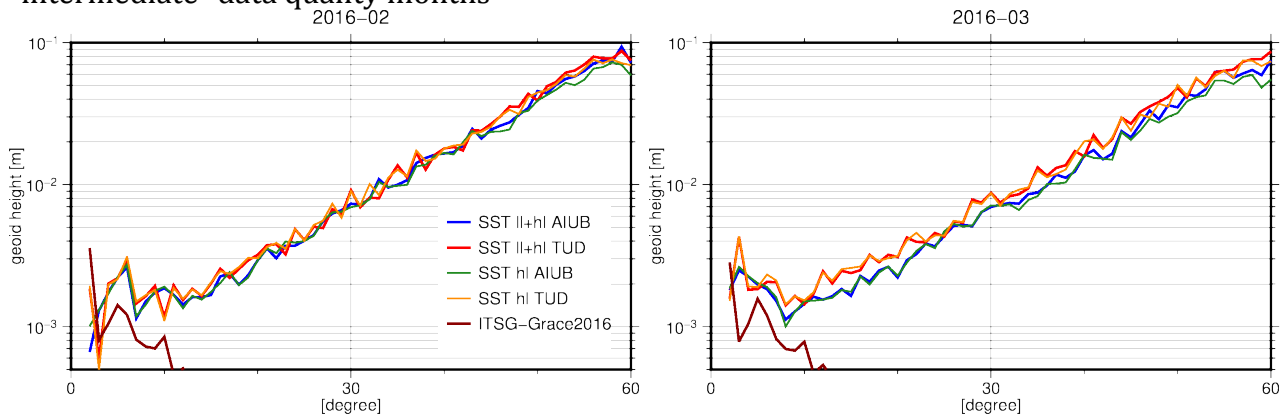


Figure 7-3: Difference degree amplitudes for all four test solutions for “intermediate” data quality test months with respect to GOCO05S (Mayer-Gürr et al., 2015).

“good” data quality months

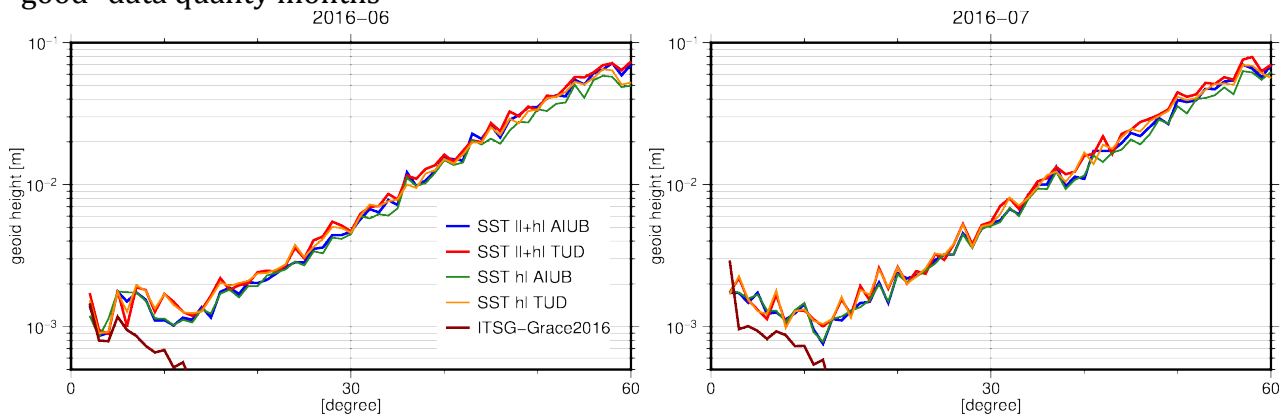


Figure 7-4: Difference degree amplitudes for all four test solutions for “good” data quality test months with respect to GOCO05S (Mayer-Gürr et al., 2015).

To see the impact on the long wavelength part of the solution we have compared the individual solutions to ITSG-Grace2016 (Mayer-Gürr et al., 2016) monthly solutions in spatial domain. The solutions are evaluated on a regular grid ($1^\circ \times 1^\circ$), reduced by the corresponding ITSG-Grace2016 monthly solution, filtered with a 500km Gaussian filter, and finally the RMS over all grid cells is computed. Table 7-1 shows the resulting RMS values for all available test months. Color codes indicate if the inclusion of the baseline data improved (green) or degraded (red) the result. It can be seen that some solutions get better and some are not. However the differences are small and all of them can be regarded as being not significant.

	TUD hl SST	TUD ll+hl SST	AIUB hl SST	AIUB ll+hl SST
01.2015	9.5	9.6	9.8	10.5
03.2015	10.9	11.1	8.4	9.6
02.2016	7.5	7.4	7.4	7.2
03.2016	8.8	8.6	7.3	7.3
06.2016	5.4	5.5	4.8	4.8
07.2016	6.7	6.5	6.3	6.1
08.2016	5.7	5.8	5.3	5.4

Table 7-1: RMS of geoid height differences [mm] on a $1^\circ \times 1^\circ$ grid for different solutions with respect to the corresponding ITSG-Grace2016 monthly solution. 500 km Gaussian filter applied.

7.4 Conclusions

We have conducted an analysis of the potential added value for gravity field inversion from KOs by including GNSS derived inter-satellite KBs. Therefore, we computed KBs between the satellites Swarm A and C for 7 test months. Two different baseline solutions computed independently by two institutes have been used. The KBs have been used to generate range observations between the two satellites, which were then introduced into the gravity field inversion process. The method used was the VEA, identical to the methodology applied for the generation of the ITSG-Grace gravity field solutions. For comparison, solutions solely based on KOs have also been produced. Comparison to the hl-only solutions and more accurate results from the ITSG-Grace2016 time series revealed that the inclusion of kinematic baselines has no impact on the final results. Solutions based on kinematic orbits already only provide the same quality. Small differences visible in the degree amplitudes or the spatial RMS can be classified as random. In general, this confirms the findings of Jäggi et al. (2009), who saw some small benefits for higher degrees when using baseline data and attributed it to the elimination of errors common to both satellites by using double-differenced observations. The new results indicate that already in the computation of the Swarm KOs common errors are mostly eliminated. Thus no improvement can be achieved by processing double-differenced data.

7.5 Bibliography

Jäggi A., Hugentobler U., Bock H., Beutler G. (2007) Precise orbit determination for GRACE using undifferenced or doubly differenced GPS data. *Advances in Space Research*, 39(10), 1612-1619, doi: 10.1016/j.asr.2007.03.012

Jäggi A., Beutler G., Prange L., Dach R., Mervart L. (2009) Assessment of GPS-only Observables for Gravity Field Recovery from GRACE. In: Sideris M.G. (eds) *Observing our Changing Earth*. International Association of Geodesy Symposia, vol 133. Springer, Berlin, Heidelberg

Multi-approach gravity field models from Swarm GPS data

SW_TN-02_ASU_GS_0001 version 1

2019-04-09

Page 44 of 44

Jäggi A., Montenbruck O., Moon Y., Wermuth M., König R., Michalak G., Bock H., Bodenmann D. (2012) Inter-agency comparison of TanDEM-X baseline solutions. *Advances in Space Research*, 50(2), 260-271, doi: 10.1016/j.asr.2012.03.027

Mayer-Gürr, Torsten; Behzadpour, Saniya; Ellmer, Matthias; Kvas, Andreas; Klinger, Beate; Zehentner, Norbert (2016): ITSG-Grace2016 - Monthly and Daily Gravity Field Solutions from GRACE. GFZ Data Services. <http://doi.org/10.5880/icgem.2016.007>

Mayer-Gürr, T., Rieser, D., Zehentner, N., Kvas, A., Klinger, B., Pail, R., Gruber, T., Fecher, T., Rexer, M., Schuh, W.-D., Kusche, J., Brockmann, J.-M., Baur, O., Hoeck, E., Krauss, S., Jaeggi, A., 2015. The combined satellite gravity field model GOCO05s. Presented at: EGU General Assembly 2015, Vienna, Austria, Geophysical Research Abstracts, vol. 17. EGU2015-12364. <http://www.goco.eu>

Montenbruck O, Gill E (2000) *Satellite Orbits*. Springer, doi: 10.1007/978-3-642-58351-3